THE OPTIMAL PLACEMENT OF SHUTOFF RODS IN CANDU NUCLEAR REACTORS

by

CHARLES W. GORDON, B.A.Sc.

PART A: MCMASTER (OFF-CAMPUS) PROJECT*

A Report Submitted to the School of Graduate Studies
in Partial Fulfilment of the Requirements
for the Degree
Master of Engineering

Department of Engineering Physics
McMaster University
Hamilton, Ontario, Canada

November 1975

* One of two project reports: The other part is designated PART B: ON-CAMPUS PROJECT.

MASTER OF ENGINEERING (1975) MCMASTER UNIVERSITY
Department of Engineering Physics Hamilton, Ontario.

TITLE: The Optimal Placement of Shutoff Rods in CANDU Nuclear Reactors

AUTHOR: Charles W. Gordon, B.A.Sc. (Toronto)

SUPERVISOR: Dr. M.H.M. Roshd

NUMBER OF PAGES: viii, 68

ABSTRACT

The optimal placement of shutdown systems in power reactors is investigated, in particular, the placement of mechanical and liquid shut-off rods. Two CANDU reactor cores were used as a basis for evaluation. The optimal shutdown system was defined here to be one which, with the least number of rods, maximizes the reactivity depth of the system with the two most effective rods assumed to be absent. It was found that rows of rods placed parallel to the fuel channels were more effective and four of these rows were required in a simple core. For real cores where positions are limited six or seven rows were needed to obtain a large system worth. (Time analysis was not done to evaluate insertion rate and delay effects on the power transient in the case of an accident.)

ACKNOWLEDGEMENTS

The author wishes to thank the staff of Atomic Energy of Canada Limited, Power Projects, for their assistance in the research for this project and, in particular, Dr. M. Roshd for his help and guidance and A.A. Pasanen for his helpful comments.

TABLE OF CONTENTS

LIST OF TABLES

LIST OF FIGURES

1. INTRODUCTION

A nuclear reactor requires a means of shutting down or stopping the fission process. This shutdown may be for safety reasons, such as a failure in the support systems, or for maintenance, such as a scheduled outage. In most reactors emergency shutdowns are accomplished by inserting into the core very strong neutron absorbers such that the reactor core becomes subcritical and the chain reaction dies away. There are normally two shutdown systems of different design in a reactor to ensure that the reactor will be shutdown even in the case of a failure of one of the shutdown systems. The mechanisms which shut the reactor down are called Shutdown Systems (SDS).

The commercial nuclear power reactors in Canada have mechanical shutoff rods (SOR) as one of the shutdown systems. These are dropped into the core. There have been several different second SDS used in the CANDU reactors. These include dumping the heavy water moderator, as in the Pickering A reactors, and injecting a neutron poison into the moderator, as in the Bruce A reactors. The two Bruce A SDS are shown in Fig. 1.

An alternative SDS has been proposed for future 750 MWe reactors. This is a liquid shutoff rod system (LSR). With this system, a strong neutron poison in liquid form is injected into tubes in the core to shutdown the reactor. The advantage of this system is that the poison can quickly be removed and the reactor restarted promptly after the requirement to be in the shutdown state has been removed. This method

has been used by the Italians in the CIRENE reactor and the British in the prototype SGHWR at Winfrith.

Since neutrons are the key to the operation of a nuclear reactor, it is important that these neutrons are not wasted in parasitic absorptions. Each shutoff rod must have a guide tube which is permanently fixed in the core. Because of this reason which has a direct bearing on the operating cost of the nuclear power reactor, as well as because of the capital cost of providing each rod, the number of rods in the core should be minimized. Another point to consider in the placement of the SDS is that reliability considerations impose the assumption that two of the rods are not available at any given time. It is normal practice to assume that the two most effective rods are out of service. Because of these constraints, a best or optimal arrangement must be sought.

The purpose of this study was to find some general results which could be applied to SDS placement. The study also specifically deals with the SOR and LSR in future 750 MWe reactors.

2. DESCRIPTION AND TERMINOLOGY

2.1 Shutoff Rod Systems

A typical mechanical shutoff rod assembly is shown in Fig. 2.[1] The SOR element is made of a stainless steel-cadmium-stainless steel sandwich in the form of a tube approximately 4-1/2 inches in diameter. The element is pulled out of the core by means of a cable and winch arrangement and held out by an electromagnetic clutch. De-energizing the clutch releases the cable and the element falls into the core under the influence of gravity or assisted by a spring. A typical insertion time would be on the order of two seconds.[1]

A typical liquid shutdown system is shown in Fig. 3.[2] The liquid poison is injected from the bottom of the calandria by gravity or high pressure gas into approximately 4 inch diameter tubes. The poison may be either a boric acid and lithium hydroxide mixture or gadolinium nitrate. A helium cover gas is used and the pipes flushed with water when the poison is withdrawn. Insertion time depends on the head in the poison tank or the gas pressure and is typically on the order of one second.[3]

2.2 SDS Safety Analysis

A SDS must be designed to safely stop any power excursion. The final concern of all nuclear safety systems is to prevent or limit the amount of radioactivity released within the station and eventually to the public. With this in mind, the delay before the SDS is actuated, the

rate at which the reactivity is inserted and the total reactivity, or the reactivity depth of the system, are designed to limit the power excursion to acceptable levels.

In accident analysis, the worst possible system failure a SDS will have to handle is a loss of coolant accident (LOCA). Of the various possible LOCA, a break in the reactor inlet header has been determined to be the limiting case in terms of setting SDS design requirements. The results of a pipe failure sets the delay and reactivity rate requirements of the SDS and the reactivity change upon losing the coolant from the core has a bearing on the total reactivity depth required of the SDS. Thus, the design objective of the SDS is to limit the over power pulse and cause sufficiently fast power rundown that the heat generated in the fuel can be removed by the discharging coolant and later by the emergency coolant without significant sheath failure.(4)

2.3 Terminology

In evaluating the effectiveness of a shutdown system of a nuclear reactor, it must be shown that it is capable of coping with the design basis accident even when the two most effective shutoff rods, the two having the greatest reactivity depth, are out of commission.

The following terminology is used in subsequent discussions:

k = effective multiplication factor. This is the ratio of the number of fissions in any one generation to the number of fissions in the immediately preceding generation. If k is unity, a reactor is said to be critical.(5)

ρ = reactivity. The reactivity is defined by

$$\rho = \frac{k - 1}{k} \quad . \tag{2.1}$$

For a critical reactor, $\rho = 0$ and for a subcritical reactor, where the flux is decreasing, $\rho < 0$.

$\Delta\rho$ = reactivity depth of a system. This is the change in reactivity due to the insertion of SOR or any other reactivity control device.

One other term is introduced here, the effective worth of a SDS. This is the reactivity depth of a SDS when the two most effective rods are missing. This is the value used in safety analysis.

3. THEORY AND COMPUTER CODES

3.1 Neutron Diffusion Theory[6]

The expected number of neutrons in an element of phase space is described by the neutron density function, $n(\underline{r},E,\underline{\Omega},t)$. The expected number of neutrons at time t, in the volume element $d\underline{r}$ about $\underline{r}$ with energy in dE about E and moving in the direction represented by the cone $d\underline{\Omega}$ about $\underline{\Omega}$, is defined by

$$dN = n(\underline{r},E,\underline{\Omega},t)d\underline{r}dEd\underline{\Omega} \quad . \tag{3.1}$$

In every element of phase space, a neutron conservation equation such as

$$\frac{dn}{dt}(\underline{r},E,\underline{\Omega},t) = \sum_i S_i \quad , \tag{3.2}$$

where $dn/dt(\underline{r},E,\underline{\Omega},t)$ is the total time derivative and the S_i are all possible sources and sinks, is satisfied.

If it is assumed that all neutrons possess the same speed and also that the neutron density function is independent of the directional vector, $\underline{\Omega}$, then the density function is given by $n(\underline{r},t)$. The left hand side of the balance equation can be written as

$$\frac{dn}{dt}(\underline{r},t) = \frac{\partial n}{\partial t} + \underline{\nabla}n \cdot \underline{v} \quad . \tag{3.3}$$

Since,

$$\underline{\nabla}n \cdot \underline{v} = \underline{\nabla} \cdot n\underline{v} - n\underline{\nabla} \cdot \underline{v} \quad , \tag{3.4}$$

and velocity space is independent of position space, by introducing the

scalar neutron flux,

$$\phi = nv \quad , \tag{3.5}$$

Equation 3.3 can be written

$$\frac{dn}{dt}(\underline{r},t) = \underline{\nabla} \cdot n\underline{v} + \frac{1}{v}\frac{\partial \phi}{\partial t} \quad , \tag{3.6}$$

or

$$\frac{dn}{dt}(\underline{r},t) = -\underline{\nabla} \cdot D\underline{\nabla}\phi + \frac{1}{v}\frac{\partial \phi}{\partial t} \quad , \tag{3.7}$$

where the diffusion approximation or Fick's Law has been used and $D(\underline{r})$ is the diffusion coefficient.

Before considering the possible sources and sinks, a certain amount of energy dependence can be added. The neutron conservation equation, Equation 3.2, is assumed to apply, not only to a volume element, but also to an energy group. This is done by noting that a neutron will change energy in a collision but not position.[7]

The neutron sink,

$$S_1 = -\Sigma_R^i(\underline{r})\phi_i(\underline{r},t)d\underline{r} \quad , \tag{3.8}$$

accounts for those neutrons scattered out of the energy group i at $\underline{r}$ in $d\underline{r}$. Similarly, a source of neutrons,

$$S_2 = \sum_{\substack{j=1 \\ j\neq i}}^{k_{max}} \Sigma_{j\to i}(\underline{r})\phi_j(\underline{r},t)d\underline{r} \quad , \tag{3.9}$$

accounts for the neutrons scattered into energy group i from group j where there are k_{max} energy groups. Another source of neutrons is the fission

neutrons. If the neutrons from fission are born into group i with a probability χ_i then,

$$S_3 = \chi_i \sum_{j=1}^{k_{max}} \nu\Sigma_f^j(\underline{r})\phi_j(\underline{r},t)d\underline{r} \quad , \tag{3.10}$$

is the number of neutrons produced per second in energy group i in $d\underline{r}$ about $\underline{r}$ due to fissions induced by neutrons of all energies. The final sink for neutrons is represented by

$$S_4 = -\Sigma_a^i(\underline{r})\phi_i(\underline{r},t)d\underline{r} \quad , \tag{3.11}$$

which accounts for all neutrons in group i absorbed in $d\underline{r}$ about $\underline{r}$.

Hence, the time independent multigroup neutron diffusion equation for energy group i is written,

$$\frac{1}{v_i}\frac{\partial}{\partial t}\phi_i(\underline{r},t) = \underline{\nabla} \cdot D_i(\underline{r})\underline{\nabla}\phi_i(\underline{r},t) - \Sigma_R^i(\underline{r})\phi_i(\underline{r},t) - \Sigma_a^i(\underline{r})\phi_i(\underline{r},t)$$
$$+ \sum_{\substack{j=1 \\ j\neq i}}^{k_{max}} \Sigma_{j\to i}(\underline{r})\phi_i(\underline{r},t) + \chi_i \sum_{j=1}^{k_{max}} \nu\Sigma_f^j(\underline{r})\phi_j(\underline{r},t). \tag{3.12}$$

If the time behaviour of the neutron population is not important, but the criticality of the system is, then the time dependence can be disregarded. A neutron balance can be forced by introducing the proportionality constant or eigenvalue, λ, such that

$$\underline{\nabla} \cdot D_i(\underline{r})\underline{\nabla}\phi_i(\underline{r}) - \Sigma_R^i(\underline{r})\phi_i(\underline{r}) - \Sigma_a^i(\underline{r})\phi_i(\underline{r})$$
$$+ \sum_{\substack{j=1 \\ j\neq i}}^{k_{max}} \Sigma_{j\to i}(\underline{r})\phi_j(\underline{r}) + \chi_i \sum_{j=1}^{k_{max}} \lambda\nu\Sigma_f^j(\underline{r})\phi_j(\underline{r}) = 0 \; . \tag{3.13}$$

The eigenvalue can be related to the multiplication constant introduced in Section 2.3 by

$$\lambda = \frac{1}{k} \quad . \tag{3.14}$$

Equation 3.13 is to be solved for the reactor. Because of the complexity of a nuclear reactor, analytic solutions of the diffusion equation are not sought, but rather numerical methods are used.

3.2 Numerical Methods[8]

In solving the multigroup diffusion equation for a nuclear reactor, an added complexity arises due to the hetrogeneous nature of the core. The core has fuel channels containing coolant and fuel bundles which are made up of fuel pellets, air gap and sheath; reactivity control devices such as zone controllers and adjuster rods; flux detectors and safety devices such as shutdown systems. In addition, in the CANDU system, on-power refuelling is used so that the fuel to be simulated has undergone various burnups. All of these factors must be accounted for in the calculation.

In practice, a computer model is used for which the diffusion equations are solved. The complexity and degree of accuracy of the model depend on the type of study; a model for fuel management would be different from a model for shutdown systems. To model the reactor, a mesh is superimposed on the core and the materials specified for each cell.

For the two dimensional diffusion equation in x-y geometry, one of the rectangular unit cells is shown in Fig. 4. Using this, the following notation is introduced:

(i) quadrants, labelled 1 through 4 which may have different volumes and properties;

(ii) lengths, L, R, T, B, defined by

$$\begin{aligned} L &= x_i - x_{i-1} \ , \\ R &= x_{i+1} - x_i \ , \\ T &= y_{j+1} - y_j \ , \\ B &= y_j - y_{j-1} \ . \end{aligned} \tag{3.15}$$

(iii) coordinates, labelled a through h defined by

$$\begin{aligned} &\text{(a)} \quad (x_i + \tfrac{R}{2},\ y_j) \ , \\ &\text{(b)} \quad (x_i + \tfrac{R}{2},\ y_j + \tfrac{T}{2}) \ , \\ &\text{(c)} \quad (x_i,\ y_j + \tfrac{T}{2}) \ , \\ &\text{(d)} \quad (x_i - \tfrac{L}{2},\ y_j + \tfrac{T}{2}) \ , \\ &\text{(e)} \quad (x_i - \tfrac{L}{2},\ y_j) \ , \\ &\text{(f)} \quad (x_i - \tfrac{L}{2},\ y_j - \tfrac{B}{2}) \ , \\ &\text{(g)} \quad (x_i,\ y_j - \tfrac{B}{2}) \ , \\ &\text{(h)} \quad (x_i + \tfrac{R}{2},\ y_j - \tfrac{B}{2}) \ . \end{aligned} \tag{3.16}$$

It is assumed that the neutron balance, Equation 3.13, holds for each rectangle about a mesh point. Multiplying through by dxdy, integrating over the area and using Gauss' theorem, the leakage term becomes

$$\int_{x_i-L/2}^{x_i+R/2} dx \int_{y_j-B/2}^{y_j+B/2} dy (\underline{\nabla} \cdot D\underline{\nabla}\phi)$$

$$= \int_{pabc} D \frac{\partial \phi}{\partial n} \, d\ell + \int_{pcde} D \frac{\partial \phi}{\partial n} \, d\ell + \int_{pefg} D \frac{\partial \phi}{\partial n} \, d\ell + \int_{pgha} D \frac{\partial \phi}{\partial n} \, d\ell, \tag{3.17}$$

where $\partial\phi/\partial n$ is the normal derivative. By cancellation, the integration is over the exterior line segments only. Using a Taylor's series expansion,

$$\left.\frac{\partial\phi}{\partial n}\right|_{x=x_i+\frac{R}{2}} = \phi_x(1) + \frac{R}{2}\phi_{xx}(1) + y\phi_{xy}(1) + \ldots, \tag{3.18}$$

where,

$$\phi_x(1) = \left.\frac{\partial\phi}{\partial x}\right|_{\text{in quadrant 1}}, \tag{3.19}$$

and integrating over dy,

$$\int_a^b D\frac{\partial\phi}{\partial n}\,d\ell = D(1)\left[\frac{T}{2}\phi_x(1) + \frac{TR}{4}\phi_{xx}(1) + \frac{T^2}{8}\phi_{xy}(1)\right], \tag{3.20}$$

and

$$\int_d^e D\frac{\partial\phi}{\partial n}\,d\ell = D(2)\left[-\frac{T}{2}\phi_x(2) + \frac{TL}{4}\phi_{xx}(2) - \frac{T^2}{8}\phi_{xy}(2)\right], \tag{3.21}$$

is obtained. Continuity of current requires

$$\begin{aligned} D(1)\phi_x(1) &= D(2)\phi_x(2), \\ D(1)\phi_{xy}(1) &= D(2)\phi_{xy}(2), \end{aligned} \tag{3.22}$$

hence,

$$\int_a^b D\frac{\partial\phi}{\partial n}\,d\ell T\int_d^e D\frac{\partial\phi}{\partial n}\,d\ell = \frac{D(1)TR}{4}\phi_{xx}(1) + \frac{D(2)TL}{4}\phi_{xx}(2). \tag{3.23}$$

Continuing this over abcdefgh, and using the difference formula for

derivatives,

$$\phi_{xx}(1) = \frac{2[\phi(i+1,j) - \phi(i,j)]}{R^2} - \frac{2\phi_x(1)}{R} \quad , \tag{3.24}$$

where $\phi(i,j)$ is the flux at mesh point (i,j), the leakage term approximation is obtained,

$$\begin{aligned} -\text{Leakage} = {} & \frac{1}{2R}[TD(1) + BD(4)][\phi(i,j) - \phi(i+1,j)] \\ & + \frac{1}{2L}[TD(2) + BD(3)][\phi(i,j) - \phi(i-1,j)] \\ & + \frac{1}{2T}[RD(1) + LD(2)][\phi(i,j) - \phi(i,j+1)] \\ & + \frac{1}{2B}[RD(4) + LD(3)][\phi(i,j) - \phi(i,j-1)]. \end{aligned} \tag{3.25}$$

Axial leakage in the two dimensional problem can be accounted for by introducing the axial buckling, B^2. In this case, the axial leakage term would be represented by

$$\begin{aligned} -\text{Axial Leakage} = {} & D(1)B^2(1)\frac{TR}{4}\phi(i,j) + D(2)B^2(2)\frac{TL}{4}\phi(i,j) \\ & + D(3)B^2(3)\frac{BL}{4}\phi(i,j) + D(4)B^2(4)\frac{BR}{4}\phi(i,j). \end{aligned} \tag{3.26}$$

This allows the buckling to be both composition and energy group dependent.

By integrating Equation 3.13 and neglecting axial leakage, a finite difference approximation to the two dimensional, multigroup neutron diffusion equation for energy group k at mesh point (i,j) with k_{max} energy groups is obtained:

$$\begin{aligned} & a^k_{ij}\phi_k(i+1,j) + b^k_{ij}\phi_k(i-1,j) + c^k_{ij}\phi_k(i,j+1) + d^k_{ij}\phi_k(i,j-1) \\ & \quad + e^k_{ij}\phi_k(i,j) - A^k_{ij}\phi_k(i,j) + S^k_{ij} + \lambda F^k_{ij} = 0 \ , \end{aligned} \tag{3.27}$$

where the coefficients are defined by:

$$a_{ij}^k = -\frac{1}{2R}\left[TD_k(1) + BD_k(4)\right] ,$$

$$b_{ij}^k = -\frac{1}{2L}\left[TD_k(2) + BD_k(3)\right] ,$$

$$c_{ij}^k = -\frac{1}{2T}\left[RD_k(1) + LD_k(2)\right] ,$$

$$d_{ij}^k = -\frac{1}{2B}\left[RD_k(4) + LD_k(3)\right] ,$$

$$e_{ij}^k = -\left[a_{ij}^k + b_{ij}^k + c_{ij}^k + d_{ij}^k\right] , \qquad (3.28)$$

$$A_{ij}^k = \left[\sum_a^k(1) + \sum_R^k(1)\right]\frac{TR}{4} + \left[\sum_a^k(2) + \sum_R^k(2)\right]\frac{TL}{4}$$
$$+ \left[\sum_a^k(3) + \sum_R^k(3)\right]\frac{BL}{4} + \left[\sum_a^k(4) + \sum_R^k(4)\right]\frac{BR}{4} ,$$

$$S_{ij}^k = \sum_{\substack{p=1 \\ p\neq k}}^{k_{max}} \left[\Sigma_{p\to k}(1)\frac{TR}{4} + \Sigma_{p\to k}(2)\frac{TL}{4} + \Sigma_{p\to k}(3)\frac{BL}{4} + \Sigma_{p\to k}(4)\frac{BR}{4}\right]\phi_p(i,j),$$

$$F_{ij}^k = \chi_k \sum_{p=1}^{k_{max}} \left[\nu\Sigma_f^p(1)\frac{TR}{4} + \nu\Sigma_f^p(2)\frac{TL}{4} + \nu\Sigma_f^p(3)\frac{BL}{4} + \nu\Sigma_f^p(4)\frac{BR}{4}\right]\phi_p(i,j) .$$

Equations 3.27 and 3.28 and their three dimensional analogues are the equations which are used to simulate a nuclear reactor core. By inputing a model into a computer code, the flux and eigenvalue can be found which satisfy Equation 3.27. The codes used in this study were EXTERMINATOR (2 dimensions) and CHEBY (3 dimensions). The difference between EXTERMINATOR and CHEBY apart from the number of dimensions is that in EXTERMINATOR, the mesh points are located at the corners of the mesh grid while in CHEBY, the mesh points are located at the centre of

the unit rectangle. An equation similar to Equation 3.27 can be written for CHEBY but with different coefficients.

3.3 The Computer Code EXTERMINATOR[9,10]

EXTERMINATOR is a computer program which solves the finite-difference analogues of the multigroup neutron diffusion equations in two dimensions using the EQUIPOISE method.[11] This method features:

(i) the extrapolated Liebmann scheme such that the flux for the (t+1) iteration, $\phi^{(t+1)}$, is of the form

$$\phi^{(t+1)} = \phi^{(t)} + \beta(\phi^{*(t+1)} - \phi^{(t)}) \quad , \tag{3.29}$$

involving the fluxes from the previous iteration, $\phi^{(t)}$, the algebraic solution of the finite difference equations, such as Equation 3.27, $\phi^{*(t+1)}$, and the overrelaxation coefficient, β;

(ii) estimating the eigenvalue by adding all the equations and solving for λ;

(iii) using the most recently computed values of the fluxes whenever possible and holding the value of λ constant throughout the sweep of the mesh.

If the five point difference equation of the same form as Equation 3.27, is cast into matrix form,

$$A\phi = \lambda M\phi \quad , \tag{3.30}$$

then, with certain conditions on A and M,

$$\frac{1}{\lambda}\phi = A^{-1}M\phi \ , \tag{3.31}$$

is obtained. The value of $1/\lambda$ is positive and associated with a unique vector ϕ.[12] In EXTERMINATOR, the matrices are partitioned and an interative procedure is set up,

$$\phi^{(t+1)} = \beta(V - \beta L - \beta\lambda_t W)^{-1}(\lambda_t M - A)\phi^{(t)} + \phi^{(t)} \ , \tag{3.32}$$

and

$$\lambda_t = \frac{e^T A\phi(t)}{e^T M\phi(t)} \ , \tag{3.33}$$

where

V = diagonal matrix of the diagonal elements of M;

L = matrix whose elements are zero except for those below the diagonal which are the negative of the corresponding elements of A;

W = matrix whose elements are zero except for those below the diagonal which are the same as the corresponding elements of M;

and e^T = row matrix all of whose elements are unity.

The program allows for several accelerating techniques. In addition to the overrelaxation technique, Equation 3.29, the program will use an "exponential β" overrelaxation if the convergence is greater than 0.1%. The exponential β scheme uses

$$\phi^{(t+1)} = \phi^{(t)}\exp\left[-\beta\left|\frac{\phi^{*(t+1)}}{\phi^{(t)}} - 1\right|\right] \ , \text{ for } \frac{\phi^{*(t+1)}}{\phi^{(t)}} - 1 < 0,$$

$$\phi^{(t+1)} = \phi^{(t)}\left\{2 - \exp\left[-\beta\left|\frac{\phi^{*(t+1)}}{\phi^{(t)}} - 1\right|\right]\right\} \ , \text{ for } \frac{\phi^{*(t+1)}}{\phi^{(t)}} - 1 > 0, \tag{3.34}$$

rather than Equation 3.29. Another method used is the extrapolation of fluxes. If the flux is converging slowly and smoothly, an Aitken δ^2 process is used to find the flux. If the flux at iteration t is converging as,

$$\phi^{(t)} = \phi^{(\infty)} + R\sigma^n \quad , \tag{3.35}$$

then,

$$\phi^{(\infty)} = \phi^{(t)} + \frac{\sigma}{1 - \sigma} (\phi^{(t)} - \phi^{(t-1)}) \quad . \tag{3.36}$$

The code calculates σ using

$$\sigma = \frac{\phi^{(t)} - \phi^{(t-1)}}{\phi^{(t-1)} - \phi^{(t-2)}} \quad . \tag{3.37}$$

This extrapolation brings the flux closer to the unique value associated with the problem. The value of β for both relaxation schemes is calculated and adjusted by the code.

Another technique to improve the iteration procedure is line relaxation as opposed to point relaxation. In line relaxation, the fluxes for a row or column in a given group are calculated from those of adjacent rows or columns and from the fluxes on the same line in other groups. Another feature of the code is a group rebalancing facility which finds the number by which the group flux is multiplied to achieve a neutron balance in each energy group as well as over all groups.

The flux is said to have converged when the convergence criteria are less than those specified by the user which, in this study, was 10^{-4}. The convergence criteria for the flux, $\epsilon_t(\phi)$, and the eigenvalue, $\epsilon_t(k)$, at iteration t, are given by

$$e_t(\phi) = \left(\frac{\phi^{(t)} - \phi^{(t-1)}}{\phi^{(t-1)}}\right)_{max} , \tag{3.38}$$

and

$$e_t(k) = \left|\frac{\lambda_t^{-1} - \lambda_{t-1}^{-1}}{\lambda_{t-1}^{-1}}\right| . \tag{3.39}$$

The axial leakage in a two dimensional problem is described by the axial buckling. EXTERMINATOR allows for the input of constant, group dependent or composition dependent buckling. Position dependent buckling can be input by specifying different compositions which vary with position only with respect to the value of the buckling.

EXTERMINATOR has many other features and options which were not used in this study.

3.4 The Computer Code CHEBY

CHEBY solves the two group neutron diffusion equations in three dimensions. CHEBY was written specifically for the CANDU type reactors and hence the neutron spectrum is divided only into fast and slow energy groups. Cross sections are calculated by cell codes and are properly weighted such that all fissions are initiated by slow neutrons and all fission produced neutrons are born into the fast group. In terms of the fast and slow neutron fluxes, ϕ_F and ϕ_S, the equations solved are

$$\begin{aligned} -\underline{\nabla} \cdot D_F \underline{\nabla}\phi_F + \Sigma_R^F \phi_F + \Sigma_a^F \phi_F &= \lambda\nu\Sigma_F^S \phi_S , \\ -\underline{\nabla} \cdot D_S \underline{\nabla}\phi_S + \Sigma_a^S \phi_S &= \Sigma_R^F \phi_F . \end{aligned} \tag{3.40}$$

To calculate the flux, the finite difference approximation is

used. In the interval, h_o, and two adjacent intervals, h_+ and h_-,

$$(\underline{\nabla} \cdot D\underline{\nabla}\phi) = \frac{2D_oD_+}{h_oD_+ + h_+D_o}(\phi_+ - \phi_o) + \frac{2D_oD_-}{h_oD_- + h_-D_o}(\phi_- - \phi_o), \quad (3.41)$$

since

$$(D\underline{\nabla}\phi)_+ = \left(\frac{h_o + h_+}{\frac{h_o}{D_o} + \frac{h_+}{D_+}}\right)\left(\frac{\phi_+ - \phi_o}{\frac{h_o + h_+}{2}}\right) + \ldots \quad (3.42)$$

Then, in three dimensions about the point (i,j,k), the fast leakage is given by

$$\begin{aligned} FL + FG\phi_F(i,j,k) &= 2[A\phi_F(i+1,j,k) + B\phi_F(i-1,j,k) + C\phi_F(i,j+1,k) \\ &+ D\phi_F(i,j-1,k) + E\phi_F(i,j,k+1) + F\phi_F(i,j,k-1)] \\ &- 2(A + B + C + D + E + F)\phi_F(i,j,k) , \end{aligned} \quad (3.43)$$

where

$$A = \frac{D_oD_+}{X_oD_+ + X_+D_o} A_{YZ} , \quad (3.44)$$

where A_{YZ} is the cross sectional area in the yz plane (and the other coefficients are of the same form).

Equation 3.40 can be written as

$$\begin{aligned} FL - FG\phi_F(i,j,k) - FA_o\phi_F(i,j,k) - FR_o\phi_F(i,j,k) + \frac{FP_o}{KE}\phi_S(i,j,k) = 0, \\ SL - SG\phi_S(i,j,k) - SA_o\phi_S(i,j,k) + FR_o\phi_F(i,j,k) = 0 , \end{aligned} \quad (3.45)$$

where the coefficients for the fast group are given by

$$FL = 2[A\phi_F(i+1,j,k) + B\phi_F(i-1,j,k) + C\phi_F(i,j+1,k)$$
$$+ D\phi_F(i,j-1,k) + E\phi_F(i,j,k+1) + F\phi_F(i,j,k-1)] ,$$
$$FG = 2[A + B + C + D + E + F] ,$$
$$FA_o = \sum_a^F(i,j,k)V(i,j,k) , \qquad (3.45)$$
$$FR_o = \sum_R^F(i,j,k)V(i,j,k) ,$$
$$FP_o = \nu\sum_f^S(i,j,k)V(i,j,k) ,$$

where V(i,j,k) is the volume of the cell centred about (i,j,k) and similar definitions apply for the slow group. The fluxes can then be written in the form

$$\phi_F(i,j,k) = \left[\frac{FL + \frac{FP_o}{KE}\phi_S(i,j,k)}{FG + FA_o + FR_o} - \phi_F(i,j,k)\right]\beta + \phi_F(i,j,k),$$
$$\phi_S(i,j,k) = \left[\frac{SL + FR_o\phi_F(i,j,k)}{SG + SA_o} - \phi_S(i,j,k)\right]\beta + \phi_S(i,j,k) , \qquad (3.46)$$

where 1/KE is the eigenvalue and β is the overrelaxation parameter. This is the Gauss Method in numerical analysis. The convergence criterion used for CHEBY in this study was 5×10^{-4} and the value of β was 1.6. Flux extrapolation and other accelerating techniques are also used.

CHEBY, in addition to finding the multiplication factor, k, and the two group fluxes, ϕ_F and ϕ_S, also has the facility to calculate bundle powers in the core. By inputing the heat generated per unit flux, bundle dimensions and the reactor power, the code will calculate the bundle and channel powers. Using this, it is possible to calculate the form factors of the reactor:

$$\text{Radial Form Factor} = \frac{\text{Average channel power}}{\text{Maximum channel power}} ,$$

$$\text{Overall Form Factor} = \frac{\text{Average bundle power}}{\text{Maximum bundle power}} , \qquad (3.47)$$

$$\text{Axial Form Factor} = \frac{\text{Overall Form Factor}}{\text{Radial Form Factor}} .$$

This is important in determining the flatness of the flux.

Since CHEBY is a three dimensional code, the reactor model used is closer to the actual system and the results are expected to be closer than those of the actual system. The disadvantage of this code with respect to EXTERMINATOR is the time required for solution, five times as long. This is the reason both codes were used.

4. INTRODUCTORY STUDIES

4.1 Use of Simple Two Dimensional Models

Before considering actual SDS configurations, some preliminary studies were done to evaluate the effects of placing various "black cells" in the core. A cell is black if every neutron crossing the surface is absorbed. The first study was to determine what could be considered a black cell. To do this, the size and the thermal absorption cross section were varied. The second study involved the interaction of black cells. The purpose of this study was to determine what configuration of black cells would divide the core into separate regions. In the final study, various black walls were placed within a core to evaluate an optimal placement.

The two dimensional code, EXTERMINATOR, with two neutron energy groups was used with a model based on a cylindrical core. In the first two studies a transversal cross section (x-y) of the core was considered while in the last study the x-z plane was used. In simulating a reactor core in both two and three dimensions, the effects of reactivity devices are smeared over a larger volume. This is done for two reasons. (i) In deriving the diffusion equation, Equation 3.13, Fick's Law was used. One of the assumptions for Fick's Law to be strictly valid is that the flux be a slowly varying function of position so that the higher order terms of a Taylor's series expansion of the flux are small.[5] In a strongly absorbing medium, the flux tends to vary rapidly and hence diffusion theory would not yield accurate results. (ii) By smearing the reactivity

devices over a larger volume, the modelling of the core is simplified.

In actual studies, the smearing is accomplished using another computer code using a supercell method. The reactivity device is smeared over a volume one lattice pitch by one lattice pitch by one bundle length. The code smears the device such that the smeared total neutron cross sections yield the same results as the accurate cell. In this way the cross sections used in all simulations were obtained.

4.2 Black Cell Study

The purpose of this study was to determine the effects on the core of varying the properties of a cell and determining what could be considered a black cell. The size of the cell and the thermal absorption cross section, $\sum_a^2$, were varied. Using symmetry boundaries, one quarter of the transversal cross section of a cylindrical core was simulated. The model used is shown in Fig. 5 along with the locations of the various black cells. Two burnup zones were assumed to account for the equilibrium fuel loading pattern in a CANDU reactor.

The results are given in Fig. 6. $\bar{\phi}_{2cell}$ is the average thermal flux in the cell and $\phi_{2centre}$, the thermal flux at the centre of the core; thus, the change in $\bar{\phi}_{2cell}/\phi_{2centre}$ is a measure of the perturbation of the flux introduced in the cell region. As shown in Fig. 6, both the change in reactivity, $\Delta\rho$, and $\bar{\phi}_{2cell}/\phi_{2centre}$ tend to level out quite rapidly with increasing cross section, $\delta\sum_a^2/\sum_a^2$. For a 3 x 3 lattice pitch cell, the value of $\bar{\phi}_{2cell}/\phi_{2centre}$ decreases by 80% when $\sum_a^2$ is doubled but falls only another 14% when $\delta\sum_a^2/\sum_a^2$ is increased a factor of five. The core becomes decreasingly sensitive to variations in the

absorption cross section as the cell becomes blacker. For a given cross section, as the size of the cell is increased the effects on the core increase. For a cell with the cross section twice normal, there is an increase from 1 x 1 lattice pitch to 2 x 2 lattice pitches.

These results for determining what to use as a "black cell" were important for later studies. It was found that a 1 x 1 lattice pitch cell reached 50% of infinite blackness when the cross section of a normal cell was doubled ($\delta\sum_a^2/\sum_a^2 = 1.0$). In the following studies a "black cell" was taken as a cell one pitch by one pitch by one bundle length, the size used in practice, with the normal cross section doubled. This cell approximates the cross sections used in the simulation of shut off rod regions.

4.3 Black Wall Study

The second set of cases was run to determine what arrangement of cells could approach the effectiveness of a black wall. It was assumed that a black wall would uncouple reactor sections and hence an infinite black wall was defined as one which gave a zero flux boundary. In this study the same model was used as in Section 4.2. To model the infinite black wall, a zero flux condition was imposed where the black wall would be. The approximation to the black wall consisted of a row of black cells as defined in the previous study. What was to be determined was how close the cells need to be in order to be considered a black wall.

A quarter core reference case with symmetry boundaries and two burnup zones was used to evaluate $\Delta\rho$ and infinite black wall cases with

zero flux boundaries were also run. Two sets of cases were examined, in the first, the core was split into half and in the second, into quarters. To evaluate the black wall approximation, the separation between the black cells was used as a parameter. It was found that the cells in the reflector had little weight and so no black cells were placed there. For the one black wall case a 1 x 1 lattice pitch size was used. For the two black wall case, two cell sizes were used, 1 x 1 and 2 x 2 lattice pitches.

The results are shown in Fig. 7. As the separation decreases, the number of poisoned cells increases and the reactivity approaches the infinite case. In Fig. 7(a), the two lattice pitch separation gives 80% of the infinite black wall reactivity. For the two black wall case, the 1 x 1 lattice pitch cell at two pitch separation yields 69% of the infinite black wall reactivity and the 2 x 2 cell with three pitch separation yields 85% of the infinite wall reactivity effect. As the separation increases, the effects tends to zero.

An interesting effect is that the "infinite black wall" simulated by a zero flux boundary gives less reactivity effect than a wall of poisoned cells. Although there is a decrease in leakage into the region, the effect of absorbing neutrons in the poisoned cells is greater. Hence, the uncoupled half core is not as subcritical as a partially uncoupled but poisoned core.

4.4 Shutoff Rod Curtain Study

The purpose of this study was to determine if there is an optimum arrangement of "curtains" of SOR and if so, what is it. A very simple

two dimensional model was evaluated using EXTERMINATOR. This simplified model was used to minimize computer time for solution and reduce the number of changes needed to alter the model.

A quarter core model in the x-z plane through the centre of the core with mesh spacing 1/2 lattice pitch, 14.2875 cm, by 1/2 bundle length, 27.5 cm, was used. A reflected core with two burnup zones and no reactivity devices other than those specifically mentioned was assumed. A constant buckling of 0.25 m^{-2} was used. In Section 5.1, it will be seen that this introduces an error in the fluxes computed. It was also assumed that a row of SOR could be represented by a continuous curtain, as in Section 4.3, and these could be placed throughout the core. The material properties of the core and the curtains were based on supercell results. In terms of $\delta\sum_a^2/\sum_a^2$ introduced in Section 4.2, the SOR in the inner core was 1.019 and in the outer core, 1.026.

The study is divided into two parts, the first deals with a plain core and the second with an adjusted core. In the plain core model the only reactivity devices in the core are the SOR curtains. Using this model six arrangements of curtains were evaluated. The adjusted core assumed the presence of adjuster rods in the core and hence, some flux flattening. Using the adjusted core model, four of the six arrangements of the first part were simulated.

To evaluate the results of this study parameters are needed to decide what is the "best" placement of the curtains. It is important to have a large reactivity depth, a minimum number of rods and to have all the rods of nearly equal statistical weight. The first two are easily measured by the change in reactivity, $\Delta\rho$, and the number of

curtains. To measure the weighting of the rods, the form factor which gives a measure of the flatness of the flux is used. For the two dimensional case, the form factor, FF, is defined by

$$FF = \frac{\bar{\phi}_2}{\phi_{2max}} = \frac{\text{(average thermal flux in the core)}}{\text{(maximum thermal flux in the core)}} . \qquad (4.1)$$

The average thermal flux in the core, $\bar{\phi}_2$, is defined by

$$\bar{\phi}_2 = \frac{\int_{(core)} \phi_2 dV}{\int_{(core)} dV} , \qquad (4.2)$$

where the integral over the core does not include the reflector. Thus, $0 \leq FF \leq 1$ and the closer FF is to unity, the flatter the flux in the core.

Part A: Plain Core

Using the plain core model, six layouts were evaluated as shown, with the results, in Fig. 8 through Fig. 13. In these studies, except Layout 4, one curtain was held fixed and the separation between the curtains varied to attempt to find an optimum arrangement. In the figures, the curtain which was varied is identified by its different positions. In Layout 4 no positions were varied. Briefly, Layout 1, Fig. 8, and Layout 2, Fig. 9, had SOR curtains parallel to the fuel channels (parallel to the z axis), Layout 5, Fig. 12, and Layout 6, Fig. 13, had curtains perpendicular to the fuel channels (parallel to the x axis) and Layout 3, Fig. 10, and Layout 4, Fig. 11, had curtains in both directions.

The "best" arrangement of SOR curtains must

(i) maximize reactivity depth,

(ii) maximize the form factor,

(iii) minimize the number of curtains.

Examining the results of the six plain core layouts, there is a trade-off between reactivity depth and form factor. In some cases when one is maximum, the other is minimum while in others there are only small differences with the different separations. On the basis of the criteria above, the "best" arrangement of each layout was chosen. These are designated by * in the figures. The choice of the "best" was somewhat arbitrary. For example, in Layout 2, Fig. 9, the form factor is maximum at the 5 pitch separation but the reactivity maximized at the 4 pitch separation. Going from 4 to 5 pitches separation, 4.24% reactivity depth is lost but the form factor is increased by 24.8%. Thus, while the 4 pitch separation yields the maximum depth, the gain in a flatter flux is significant and the 5 pitch separation was chosen as "best".

Since Layout 1 has the minimum depth, minimum number of curtains and the maximum form factor, it is chosen as a basis for evaluation. In terms of this basis, the following table can be formed.

Layout i	$\frac{(\Delta\rho)_i}{(\Delta\rho)_1}$	$\frac{(FF)_i}{(FF)_1}$	$\frac{(\#\text{ of curtains})_i}{(\#\text{ of curtains})_1}$
1	1.00	1.00	1.00
2	1.41	0.88	1.33
3	1.26	0.59	1.33
4	1.62	0.57	1.67
5	1.36	0.72	1.00
6	1.39	0.45	1.33

Of the six layouts, Layout 2 and Layout 4 have the greatest depth. Layout 4 has the largest depth but it has one of the lowest form factors and the greatest number of curtains of the six cases. Layout 2 has the second largest reactivity depth and form factor of the six cases so Layout 2 is chosen as the "best" of the plain core layouts.

Part B: Adjusted Core

In a real reactor the centre peak of the flux is lowered to achieve a flatter flux in the core. This can be done using adjuster rods. In the adjusted core cases the adjusters were simulated using curtains. The curtain properties were found by averaging the supercell values (Section 4.1) over a continuous curtain. A parameter, α, was averaged to $\bar{\alpha}$ by

$$\bar{\alpha} = \frac{\int_{(\text{adjuster})} \alpha\phi dV + \int_{(\text{core}^*)} \alpha\phi dV}{\int_{(\text{adjuster})} \phi dV + \int_{(\text{core}^*)} \phi dV} \quad , \tag{4.3}$$

where (core*) represents a volume of core adjacent to and equal in volume to the adjuster rods. The placement of these adjusters was optimized and the material properties altered to give the flattest flux. The curtains were 18 lattice pitches long, separated by 1/2 bundle length. This arrangement yields a form factor of 0.71 compared to the plain core form factor of 0.51. With these adjuster curtains in the core, Layouts 1, 2, 5 and 6 were re-done and the results are given in Fig. 14 through Fig. 17.

Proceeding as in the plain core section, the results for the "best" arrangements can be written in the form of a table using Layout 1 (adjusted) as the base.

Layout i	$\frac{(\Delta\rho)_i}{(\Delta\rho)_1}$	$\frac{(FF)_i}{(FF)_1}$	$\frac{(\#\text{ of curtains})_i}{(\#\text{ of curtains})_1}$
1	1.00	1.00	1.00
2	1.41	0.67	1.33
5	1.51	0.55	1.00
6	1.61	0.39	1.33

Although Layout 5 has reasonable values, a flux map shows the thermal flux in the centre of the core is very depressed. The ratio of $\phi_{2centre}/\phi_{2max}$ is almost zero. Because of this, Layout 2 is again chosen as "best"

No clearly optimal arrangement of SOR curtains was found in this study. There must be a tradeoff between reactivity depth and form factor to determine the "best" layout. Layout 2 which consists of 4 curtains arranged parallel to the z axis (or the fuel channels) is the "best" arrangement. This is true for both the plain core and adjusted core models. The effect on the adjusters is to decrease the reactivity worth of the SOR curtains when compared to the plain core results.

5. 2-D REACTOR A MODELS

5.1 First Model: No Shutoff Rods

The first reactor studied was based on a possible 750 MWe reactor designated Reactor A. The placement of devices is shown in Fig. 18. The need to minimize the number of SOR becomes obvious when the number of devices to be inserted in the core is seen. This first two dimensional model of Reactor A simulated was a quarter core in the x-z plane. The model had 23 radial and 10 axial mesh-points and 2 energy groups. In the whole core there are 24 adjuster rods and 6 zone controllers. The purpose of the model was to find a value for the constant buckling, B^2, which would give a near critical core.

The control devices were smeared as described in Section 4.1 and the positions found as follows. The position from Fig. 18 was taken as the centre of the device and the edges of the smeared cell found by adding or subtracting half a bundle length and positioning it between the adjacent fuel channels. The bundle length for this core was 49.53 cm and the lattice pitch, 28.575 cm.

The results of the cases run are summarized in the following table:

Case	$B^2(m^{-2})$	k	ρ(mk)
1	0.40	0.9882	-11.94
2	0.35	0.9901	-10.00
3	0.25	0.9940	- 6.04
4	0.15	0.9980	- 2.00

As the buckling is decreased, the multiplication factor is increased. As B^2 is reduced, the axial leakage is decreased and hence neutron losses are reduced. In the second model $B^2 = 0.15\ m^{-2}$ was used which gives a 2 mk subcritical core.

5.2 Second Model: A Core With Constant Buckling

In the second model of Reactor A the SOR's were included. The positions were found in the same way the positions for the adjuster rods and zone controllers were found in Section 5.1. This model had two purposes: (1) to check the agreement between the two and three dimensional fluxes using a CHEBY simulation which was available; (2) to investigate alternative configurations of SOR.

The comparison of CHEBY and EXTERMINATOR fluxes is shown in Fig. 19 and Fig. 20. The CHEBY flux was taken at the centre z plane of the core. As can be seen, the agreement is not good. The mesh in CHEBY model with the SOR's out is finer (Fig. 19) showing the flux depression in the adjuster rods, but the EXTERMINATOR flux roughly follows the three dimensional flux introducing an error of 46% at the peak. With the SOR inserted, Fig. 20, the assumption of constant buckling seriously distorts the flux introducing an error of 270% at the flux peak. An important feature with respect to the placement of SOR is the peaking of the thermal flux in the outer core. This peaking occurs in both the CHEBY and EXTERMINATOR simulations. The peak to centre thermal flux ratio is 15.0 for CHEBY and 51.8 for EXTERMINATOR when the SOR are inserted.

The second purpose of this model was to investigate alternative

SOR placements. In placing the rods it is important not to leave large volumes which must be shutdown by one rod since this would give a large worth to that rod. Also, it is important not to group too many rods together since this tends to depress the flux too much and reduce the worth per rod. In forming alternative layouts, the arrangement must be physically realizable. By this it is meant that the SOR must not centre on a fuel channel or be located too close to any other device already located in the core.

A sketch of the SOR positions is shown in Fig. 21, along with the results. The CHEBY run referred to above yielded a system depth of -79.9 mk for the proposed layout compared to the EXTERMINATOR result of -66.5 mk which is 14.6% less. Some interesting results however came out of this analysis:

(1) Withdrawing the centre six SOR, S_8, S_9 in Fig. 21, results in a decrease of only 0.75 mk or 1.1% of the total.

(2) Shifting the outer rows of SOR out one pitch S_{1a}, S_{2a}, S_{3a} in Fig. 21, and straightening the centre row, S_{5a}, S_6, S_{7b}, increases the reactivity depth by 12.6 mk or 18.3% with the centre six rods removed.

(3) A 32 rod layout increased the depth of the SDS by 0.2 mk while decreasing the number of rods by 6%.

In the second case above, a large reactivity worth was added. This was due mainly to the distorted flux shape in the outer region which

EXTERMINATOR predicts. It is interesting to note that arranging the rods in "curtains" parallel to the z axis seems to be more effective (Section 4.4).

5.3 Third Model: A Core With Variable Buckling

This model was introduced to correct some of the error introduced by the assumption of constant buckling. In this case the feature in EXTERMINATOR which allows the assignment of different bucklings to each materials was used (Section 3.3). It was hoped that by using this, the fluxes could be correctly modelled and hence more accurate results could be obtained using only a 2-D model.

Referring to Fig. 22, an approximate set of bucklings was calculated using

$$B_i^2 = \left(\frac{\pi}{Y_i}\right)^2 \quad , \tag{5.1}$$

where i indicates the region where the buckling applies, $x_i \rightarrow x_{i+1}$, and where

$$Y_i = (R^2 - X_i)^{1/2} \quad . \tag{5.2}$$

The resultant bucklings are given in Fig. 22. The regions were divided so that the reactivity devices would not be divided into regions with different bucklings.

Using the above set of bucklings, the core with the SOR out was 25.5 mk subcritical whereas the CHEBY model was just critical. The error in the fluxes was maximum in the outer core and EXTERMINATOR underestimated the peak flux along the x direction by 19%. When the SOR were

inserted, the code overestimated the flux in the x direction by a maximum of 61% in the outer core; the flux in the z direction was underestimated by 16% and the reactivity overestimated by 8.5%. To improve the model, the bucklings were altered. When the bucklings were uniformly reduced by 0.4 m^{-2}, the core becomes 7.8 mk subcritical and the SDS worth was -82.3 mk, 5.6% greater than predicted by CHEBY. With the SOR out, the flux is underestimated by 11% in the x direction at the maximum difference in the outer core and with the SOR inserted, the flux in the outer core is overestimated by 66%. To lower the flux error in the outer core, the bucklings in the outer core were returned to the original value.

Using this new set of bucklings, the core without the SOR was 9.9 mk subcritical and the worth of the SDS overestimated by 20.7%. With the rods out, Fig. 23, the thermal flux in the x direction is underestimated by EXTERMINATOR with respect to CHEBY by 36% in the outer core, but with the SOR inserted, Fig. 24, this error is only 9.6%.

Since the bucklings depend on flux shape and this is drastically altered by inserting the SDS, it was concluded that an accurate representation of the flux without a detailed knowledge in advance is not easily accomplished. In view of this and since the last set of bucklings reasonably depicts the perturbed flux, this set was used.

Using a pattern similar to that of Section 4.4, four SOR curtains were to be located in the core parallel to the z axis. The parameter characterizing the different variations was the separation between the inner and outer curtains. The outer curtain was fixed at 8.5 pitches from the centre-line and the inner curtain allowed to vary in position.

The results are given in Table 1.

From Table 1, the "best" arrangement is reasonably clear. The case with 5 pitch separation gives maximum reactivity depth and the form factor is less than 1% less than the maximum form factor at 6 pitches separation. It is interesting to note that the more accurate model of Reactor A yields the same "best" SOR arrangement of 4 curtains as the simple model of Section 4.4. This arrangement contains only 24 rods, almost 30% less than the number of rods in the proposed layout. The layout had a total worth of -63.3 mk, 33% less than the proposed layout, and had a form factor of 0.457, 59% greater than the proposed layout. The flux is shown in Fig. 25.

The next improvement was to use a three dimensional model simulated by CHEBY.

6. 3-D CHEBY MODELS

Due to the proprietary nature of the calculations for this section, only a brief summary is given here.[13]

CHEBY models of Reactor A (Section 5.1) were simulated. The proposed and alternative SOR configurations were investigated with respect to reactivity depth, form factors and effective worth. Recall that the effective worth (Section 2.3) is the reactivity depth of the shutdown system when the two rods with the greatest statistical weight or worth are assumed to be out of action. The arrangement which was found to be better than the proposed layout, Fig. 18, consisted of seven rows of SOR arranged roughly parallel to the z axis. Since the positions available for the SOR are limited, more curtains were needed.

A second 750 MWe core, Reactor B, was also simulated. This core contained 24 adjuster rods, 30 mechanical shutoff rods and 32 liquid shutoff rods. This core is shown in Fig. 26. The proposed LSR arrangement gave reasonable results and so no further alternative layouts were investigated. Alternative SOR layouts were investigated and it was found that placing rows of SOR in the outer core and bending the rows in the centre region gives "best" results. These curtains were not as clearly defined as in previous results but with the LSR system also in the core, there are far fewer positions available for the SOR. Nonetheless, the curtains tend to be concentrated in the outer edges and parallel to the z axis. Also it was found that portions of the SOR which extend into

the reflector could be neglected since this is a region of low neutron importance.

7. CONCLUSIONS

On the basis of this limited study, general rules applicable to all reactors cannot be formulated. This study involved only two similar CANDU reactor cores, and hence, the results have a limited data base. Some useful points, however, have been brought out.

The optimal placement of shutoff rods was defined as the one which, with the minimum number of rods, maximizes the reactivity depth and minimizes the worth of the two best rods. This, however, was not easy to achieve. In the simple core studied, most of the layouts which maximized the reactivity depth did not also maximize the form factor.

When the shutoff rods are arranged in curtains or rows which separate the core into regions, the results obtained depend greatly on the positions of the curtains. This means that when a shutdown system is designed, the shutoff rods cannot be placed in convenient gaps if a reasonably good arrangement is to be formed. The arrangement of rows will depend on the reactor and on the placement of the other reactivity devices. For the particular cores studied, arranging the rows of shutoff rods parallel to the z axis, that is, parallel to the fuel channels, gives the "best" results. Since the adjusters form rows along the x direction, and these tend to separate the core into regions, splitting the core into smaller volumes using curtains parallel to the z direction might be the more effective layout. It was also found that for a plain core, one without adjusters, the curtains parallel to the z direction

were the most effective layout as well. This could be explained by the fact that the flux and importance drops off in the z direction faster than in the x direction.

From the results of the simple two dimensional models, four curtains arranged parallel to the fuel channels formed the "best" SDS in both the plain core and the adjusted core. This divides the core into five partially coupled regions. In the more accurate models in three dimensions, the "best" layout required more curtains since the positions available for the rods were limited. Generally six or seven rows were needed with more rods in the outer regions to reduce flux peaking. The rows were not necessarily in a straight line but some were bowed towards the outer core near the centre. Also, it was found that sections of shutoff rods which extended into the reflector could be removed without a great loss of reactivity depth.

Only static simulations were made in these studies. For a more complete shutdown system analysis the time dependence of power during a shutdown must be considered. Simulation of loss of coolant accidents in the reactor using space-time computer codes would be necessary to determine whether the delay, rate of reactivity insertion, and the depth of the optimal layout are sufficient to cope with accident conditions.

TABLE 1

Reactor A Variable Buckling 2-D Model Results for Positioning Four SOR Curtains*

Case	$\Delta\rho$(mk)	$\bar{\phi}_2/\phi_{2max}$
Reference SOR out	-	0.6010
Reference 30 SOR in	-94.017	0.2876
3 Pitch Separation	-32.986	0.2690
4 Pitch Separation	-48.309	0.2747
5 Pitch Separation	-63.344	0.4567
6 Pitch Separation	-58.287	0.4576

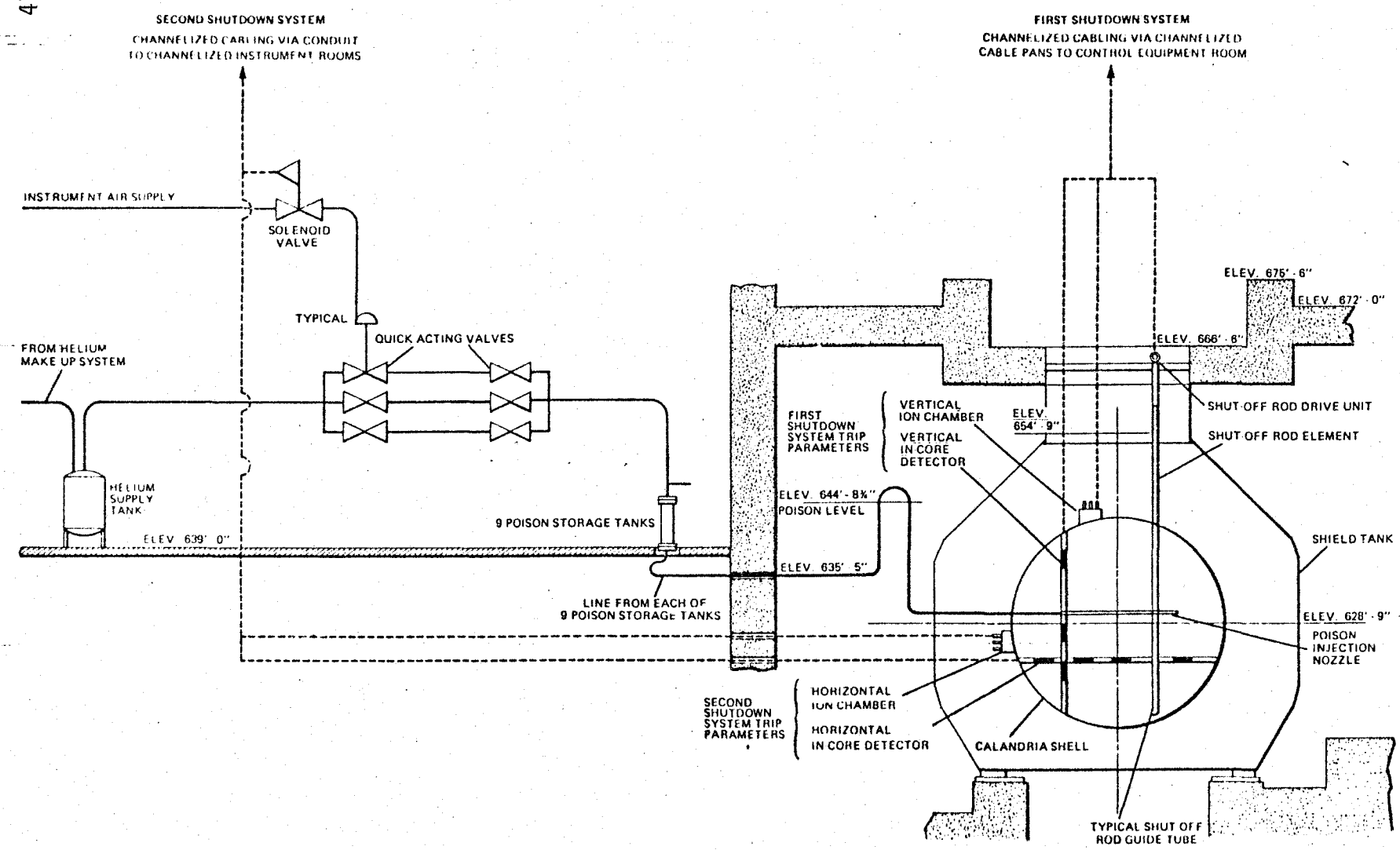

FIG. 1 BRUCE A FIRST AND SECOND SHUTDOWN SYSTEMS

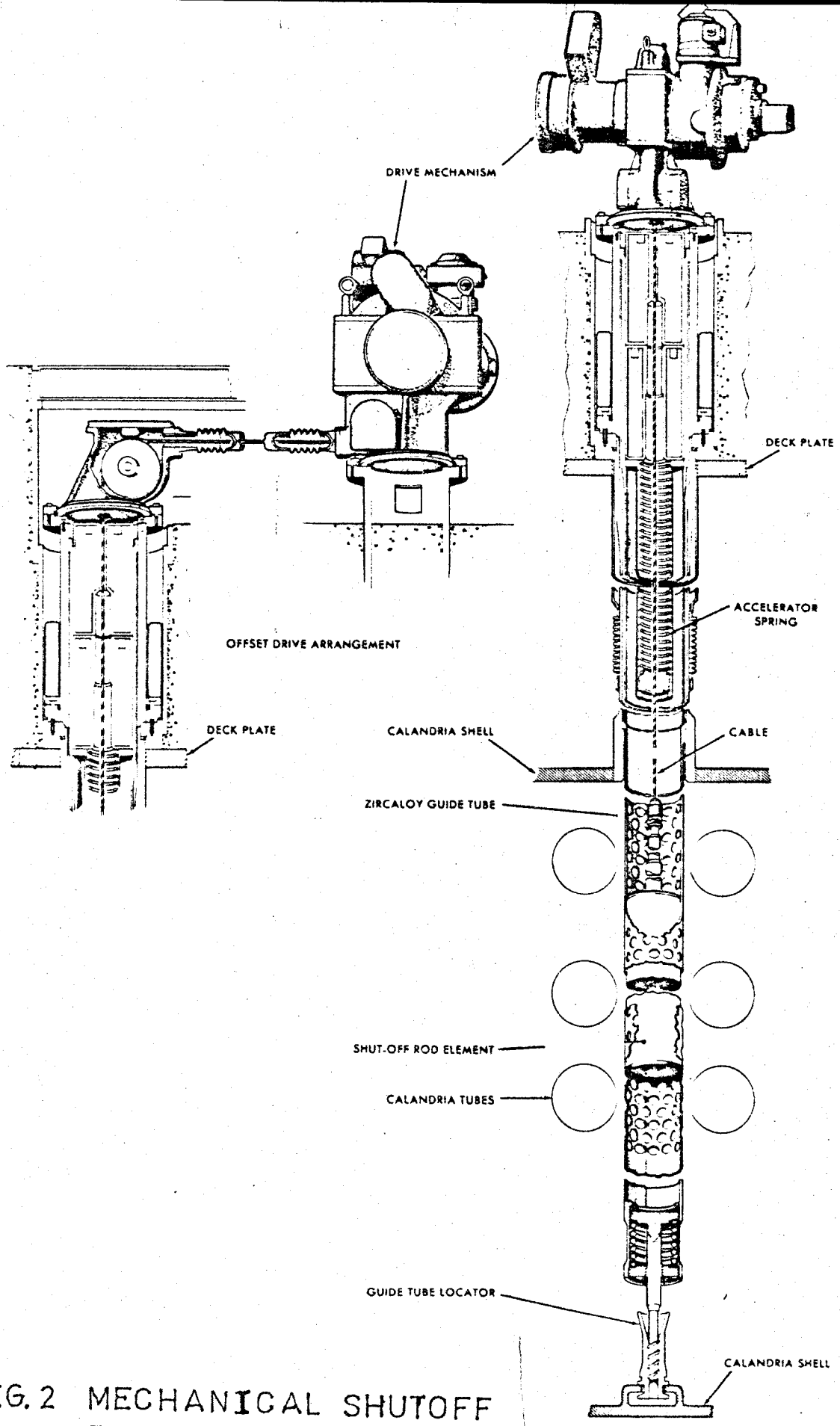

FIG. 2 MECHANICAL SHUTOFF ROD ASSEMBLY

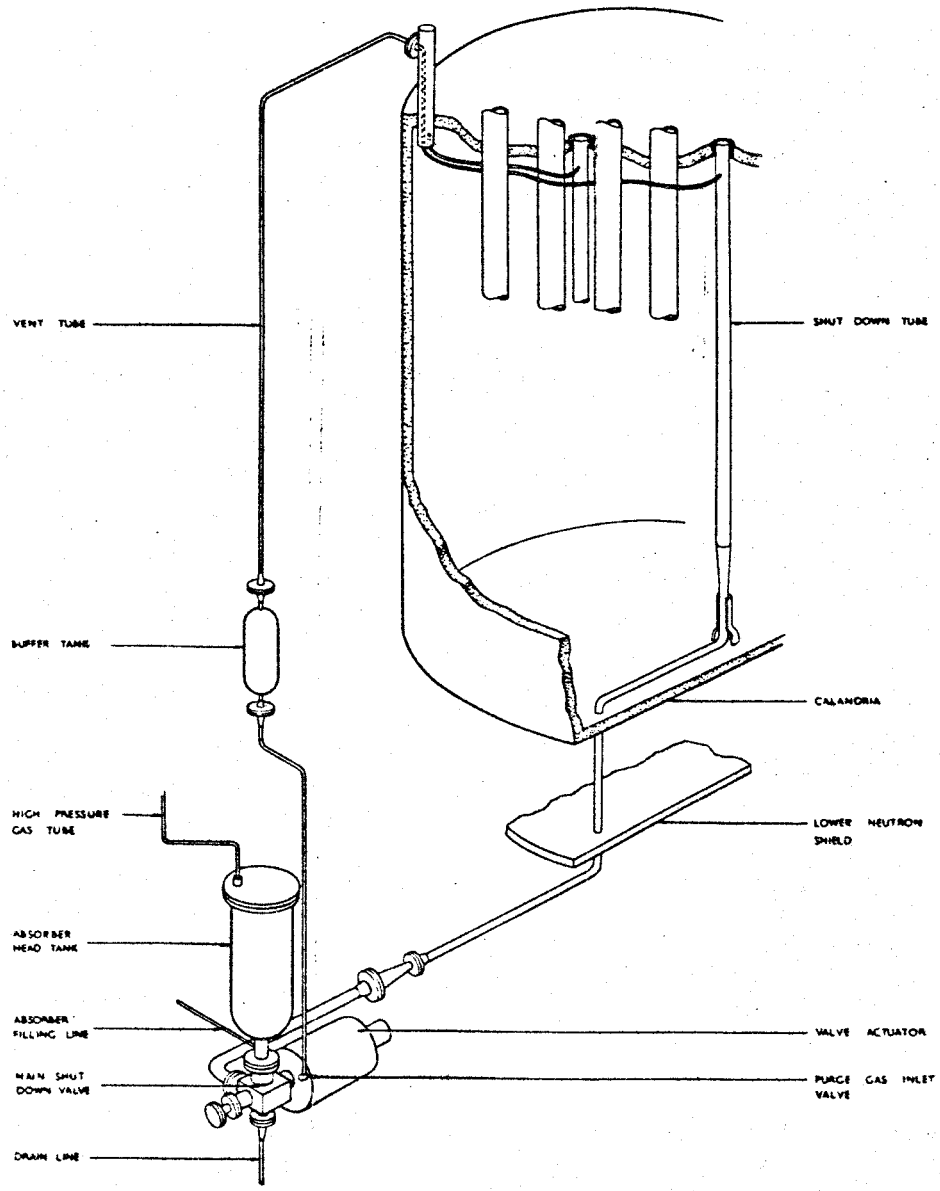

FIG. 3 LIQUID SHUTOFF ROD ASSEMBLY

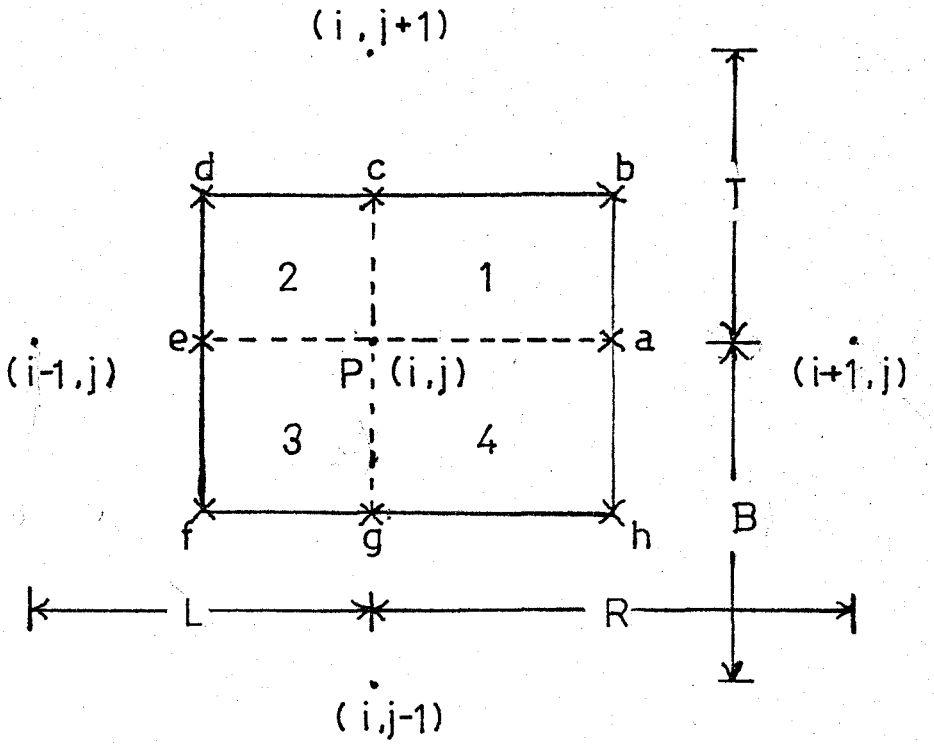

FIG. 4 FLUX POINT FOR
2-D ITERATION

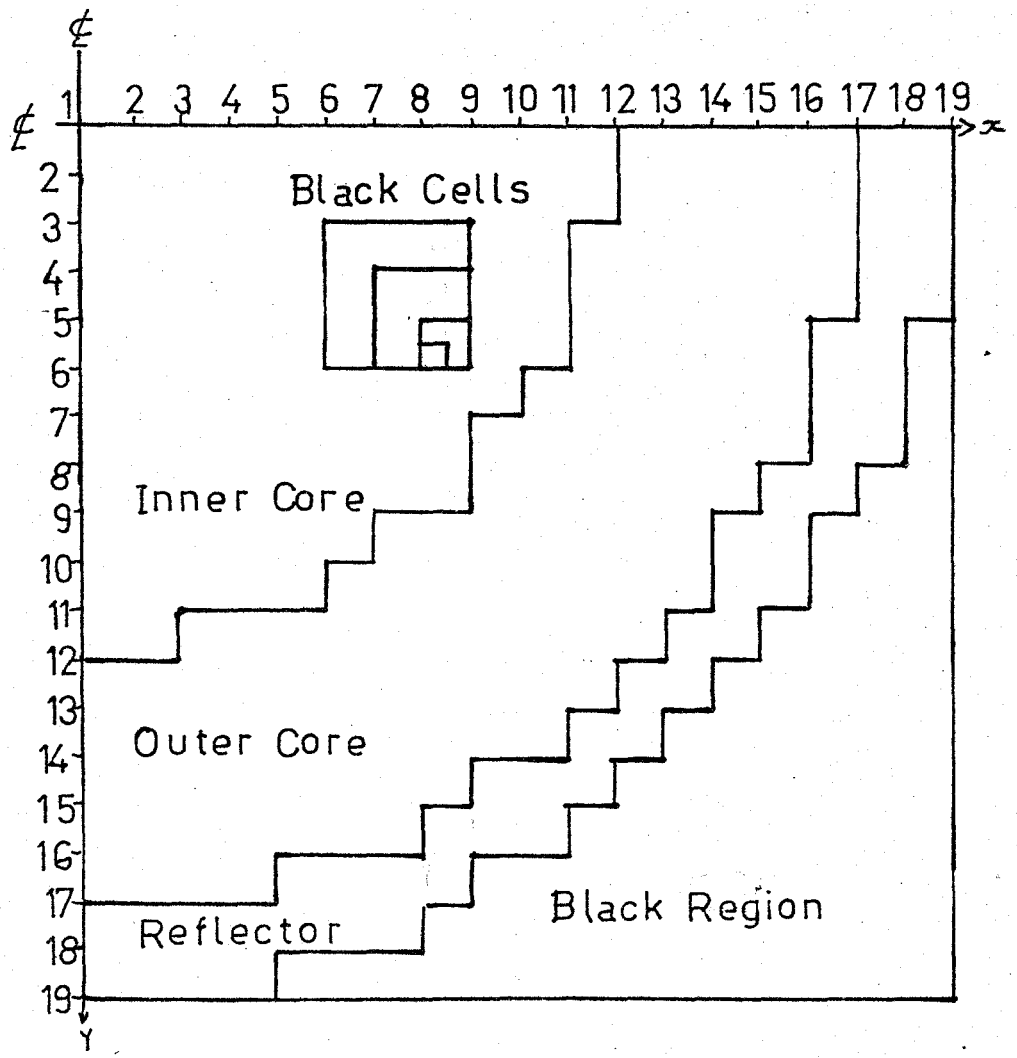

FIG 5 EXTERMINATOR
BLACK CELL - BLACK WALL
MODEL

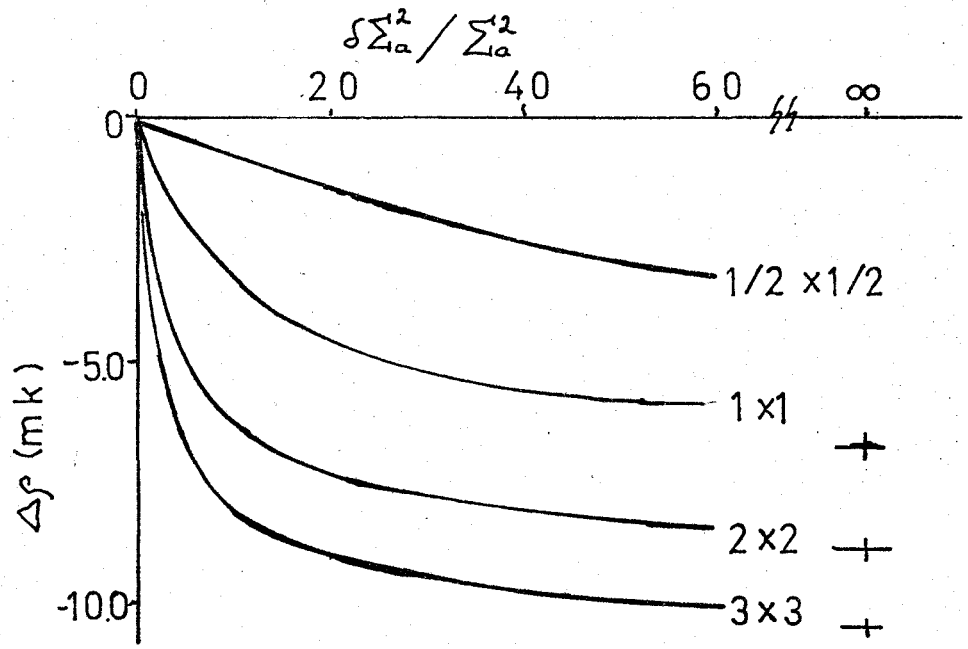

(a) Reactivity Effects

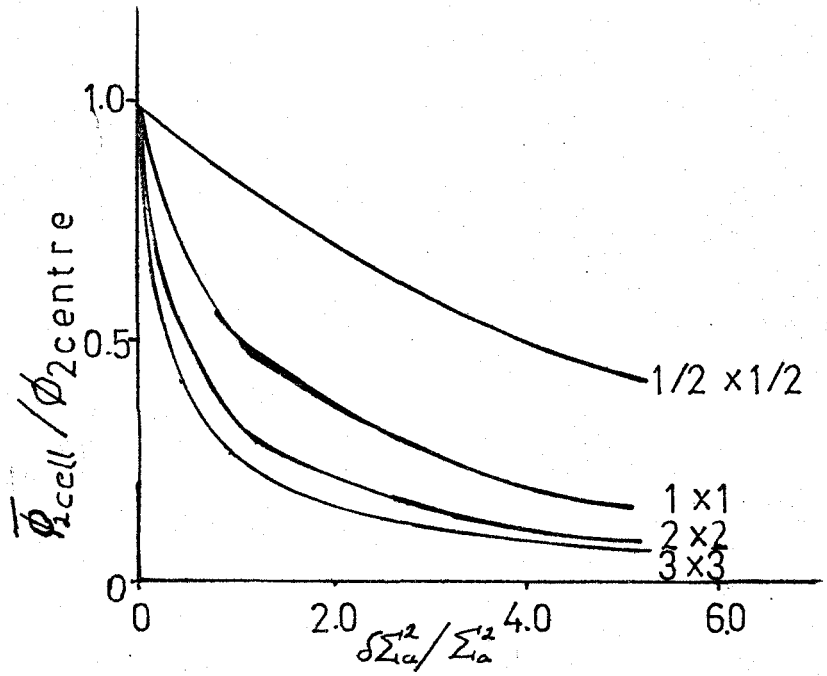

(b) Flux Depression

FIG 6 BLACK CELL RESULTS FOR VARIOUS CELL SIZES

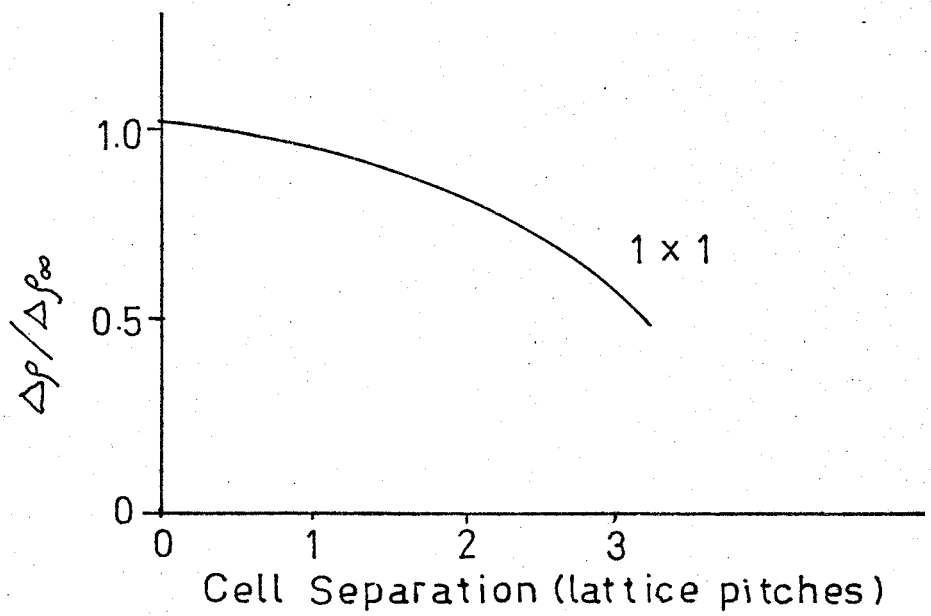

(a) One Black Wall

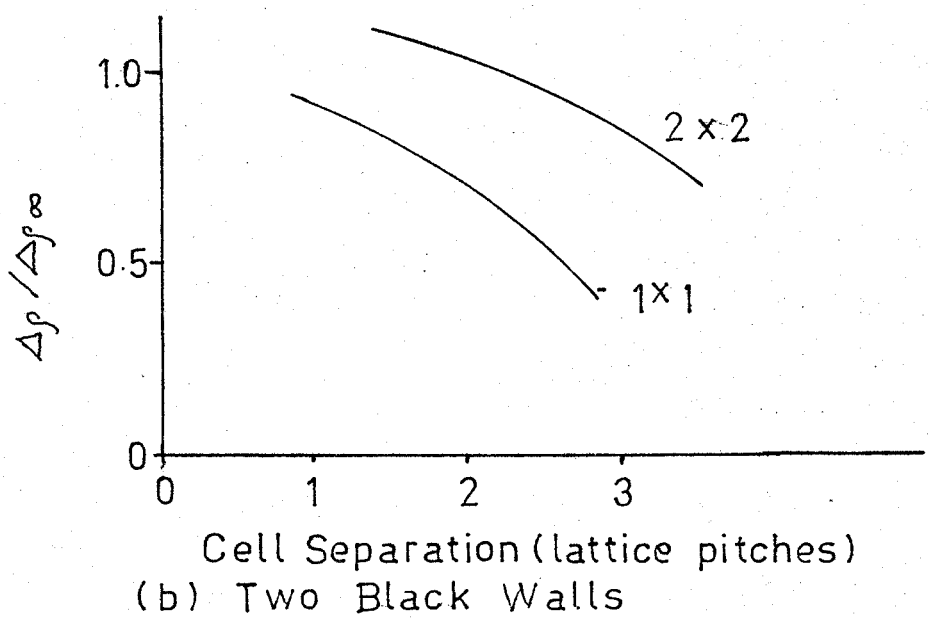

(b) Two Black Walls

FIG 7 BLACK WALL RESULTS FOR ONE AND TWO BLACK WALLS

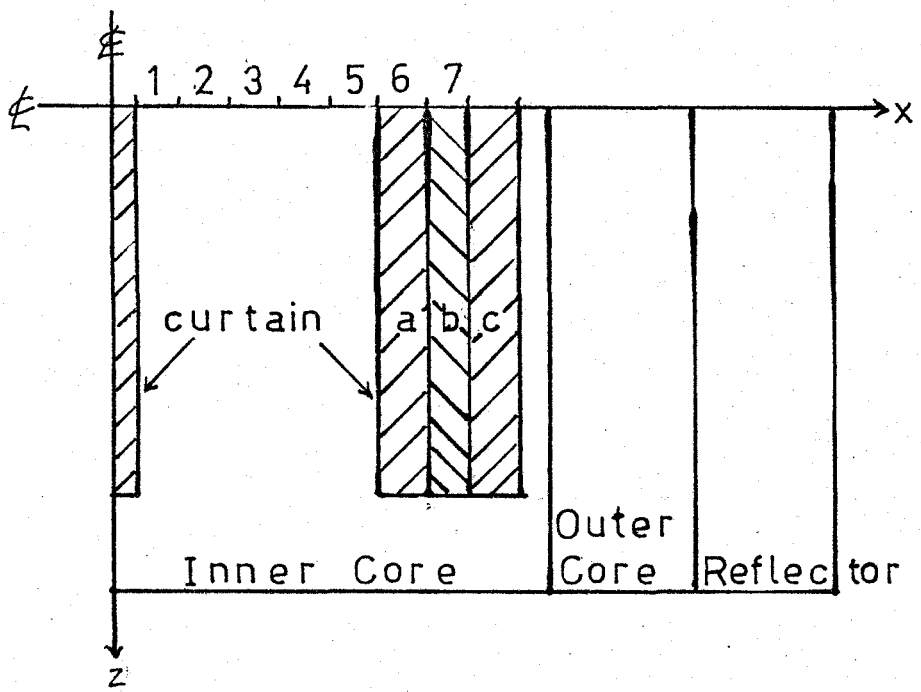

CASE	$\Delta\rho$ (mk)	ϕ_2 / ϕ_{2max}
ref	——	0.5084
a	- 51.562	0.2968
* b	- 63.743	0.4874
c	- 54.108	0.3490

FIG. 8 SOR CURTAIN STUDY, PLAIN CORE: LAYOUT 1

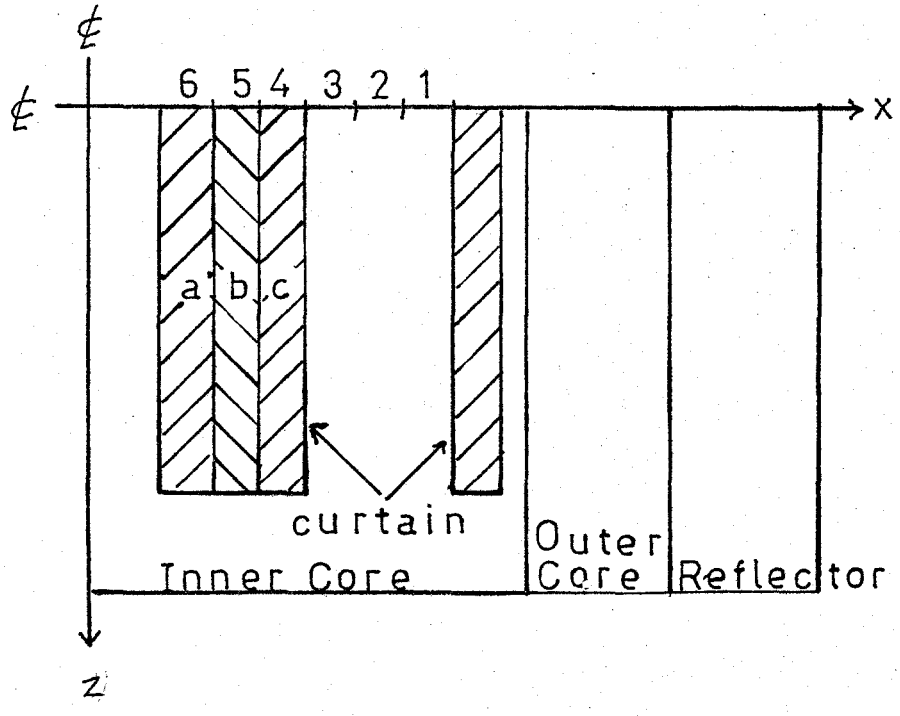

CASE	$\Delta\rho$ (mk)	$\bar{\phi}_z/\phi_{z\max}$
ref	———	0.5084
* a	-89.627	0.4313
b	-93.597	0.3455
c	-59.047	0.1790

FIG 9 SOR CURTAIN STUDY, PLAIN CORE: LAYOUT 2

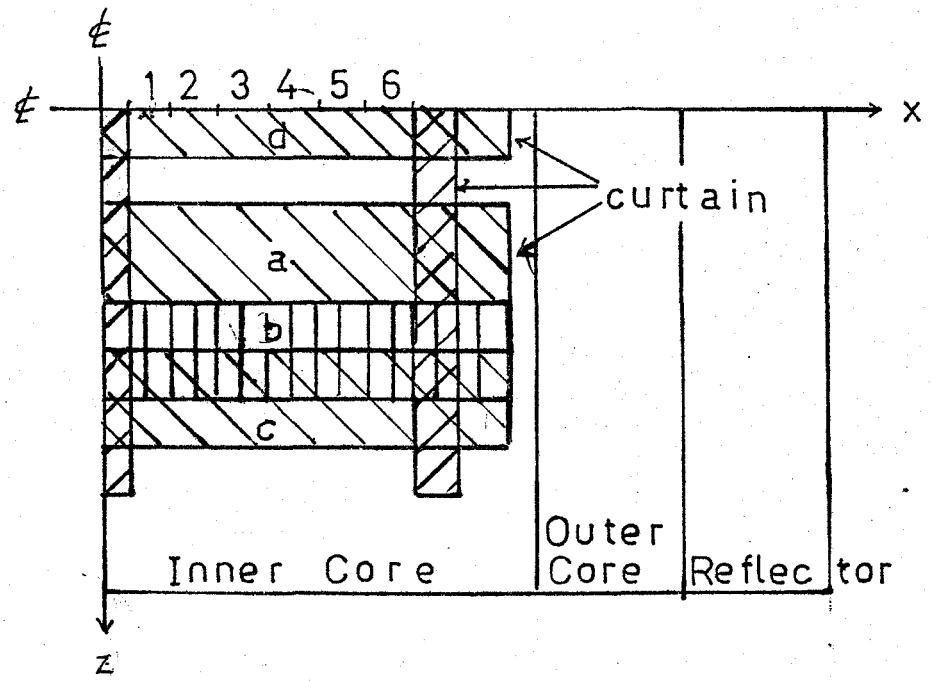

CASE	$\Delta\rho$ (mk)	$\bar{\phi}_2/\phi_{2max}$
ref	———	0·5084
a	-81·192	0·2794
b	-62·724	0·3371
c	-74·138	0·2487
* d	-80·093	0·2871

FIG 10 SOR CURTAIN STUDY. PLAIN CORE: LAYOUT 3

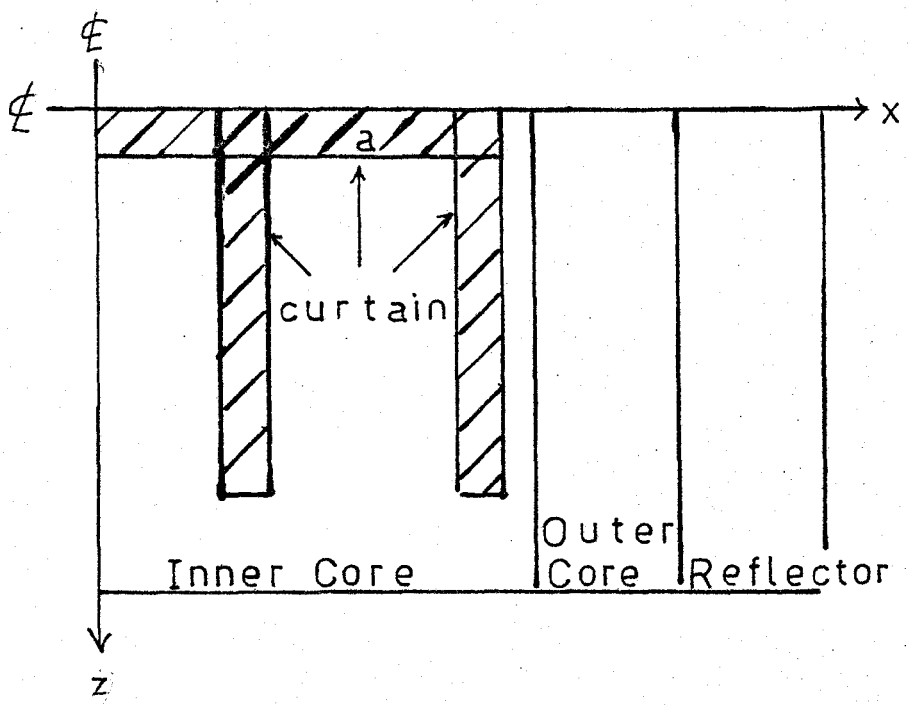

CASE	$\Delta\rho$ (mk)	$\bar{\phi}_z / \phi_{zmax}$
ref	———	0.5084
a	-103.304	0.2785

FIG. 11 SOR CURTAIN STUDY, PLAIN CORE: LAYOUT 4

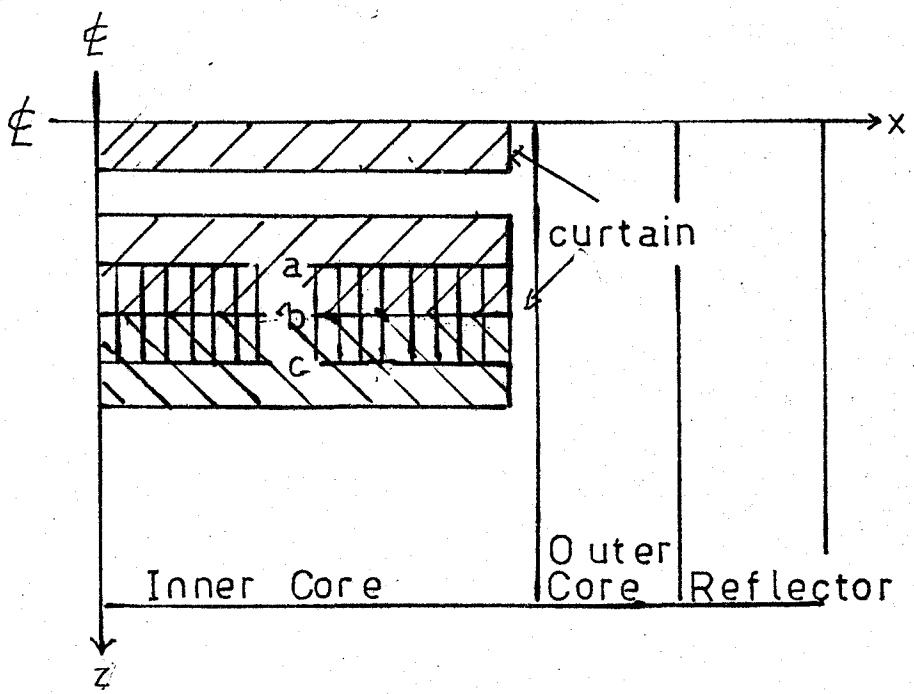

CASE	$\Delta\rho$ (mk)	$\bar{\phi}_z / \phi_{z\max}$
ref	———	0.5084
a	-79.328	0.3891
* b	-86.867	0.3511
c	-84.706	0.2276

FIG.12 SOR CURTAIN STUDY.
PLAIN CORE : LAYOUT 5

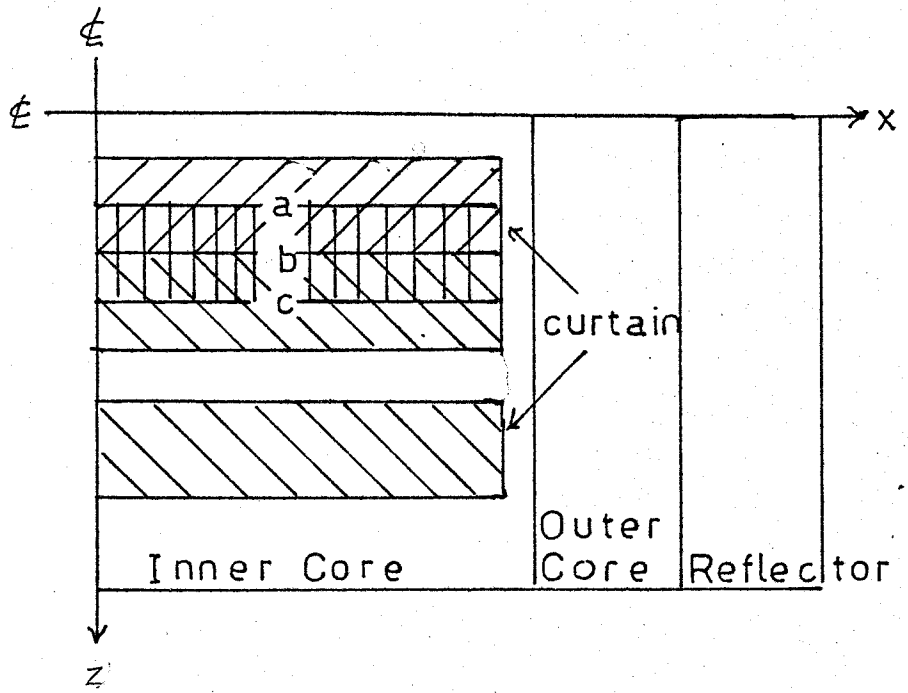

CASE	$\Delta\rho$ (mk)	ϕ_2/ϕ_{2max}
ref	———	0.5084
* a	-88.519	0.2198
b	-82.454	0.2048
c	-63.257	0.2518

FIG.13 SOR CURTAIN STUDY.
PLAIN CORE: LAYOUT 6

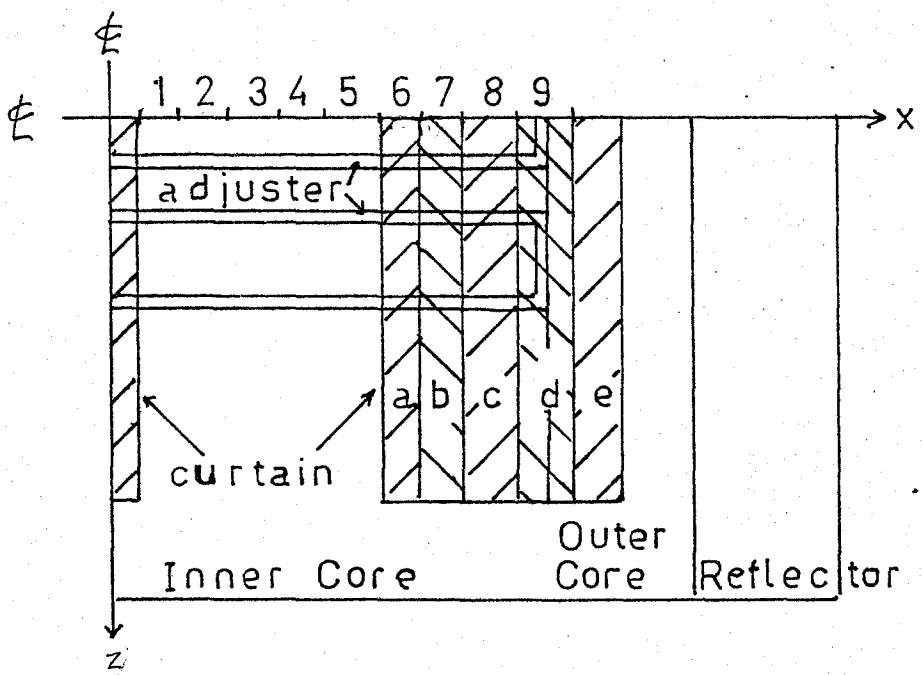

CASE	$\Delta\rho$ (mk)	$\bar{\phi}_2/\phi_{2max}$
ref		0.7090
a	- 27.187	0.2835
b	- 44.445	0.2962
* c	- 50.745	0.4877
d	- 47.252	0.4378
e	- 38.559	0.4646

FIG.14 SOR CURTAIN STUDY.
ADJUSTED CORE: LAYOUT 1

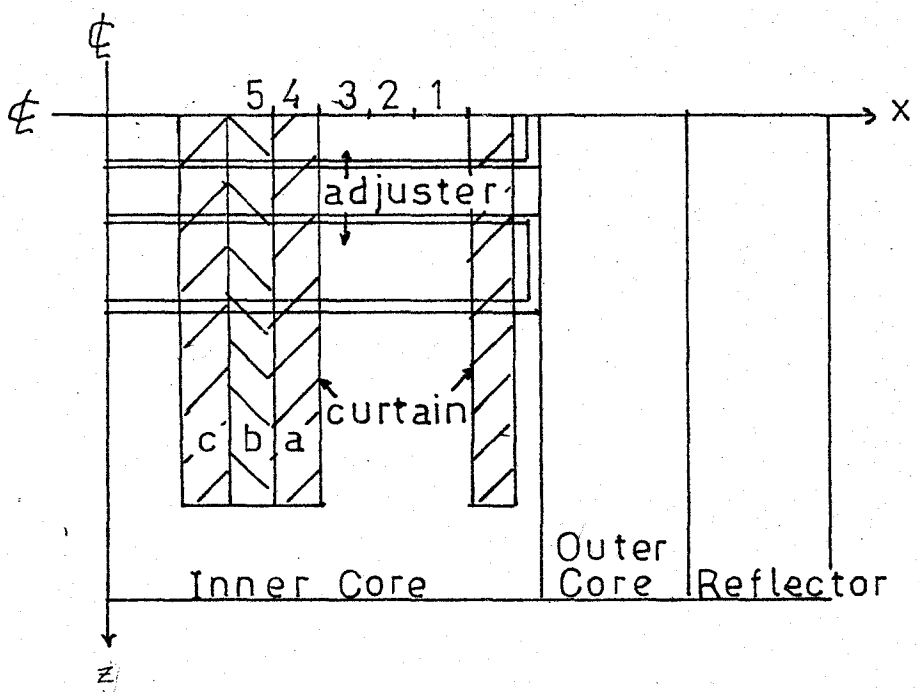

CASE	$\Delta\rho$ (mk)	$\bar{\phi}_2/\phi_{2max}$
ref	———	0.7090
a	-52.228	0.2328
b	-74.935	0.2752
* c	-71.646	0.3251

FIG. 15 SOR CURTAIN STUDY.
ADJUSTED CORE: LAYOUT 2

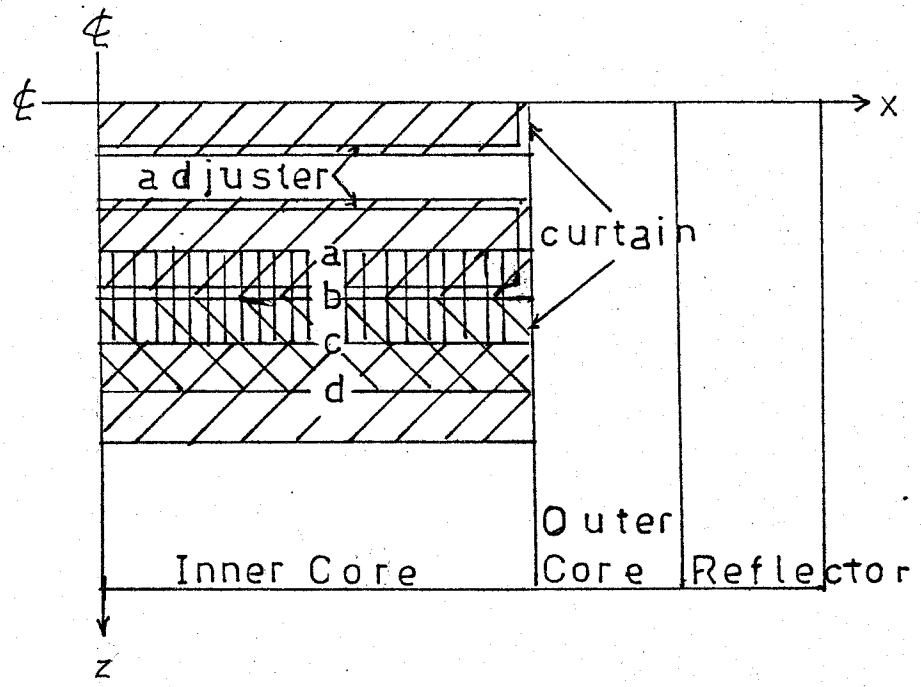

CASE	$\Delta\rho$ (mk)	$\bar{\phi}_2/\phi_{2max}$
ref	——	0.7090
a	-61.117	0.4231
* b	-76.672	0.2680
c	-77.581	0.2114
d	-70.284	0.2165

FIG. 16 SOR CURTAIN STUDY. ADJUSTED CORE: LAYOUT 5

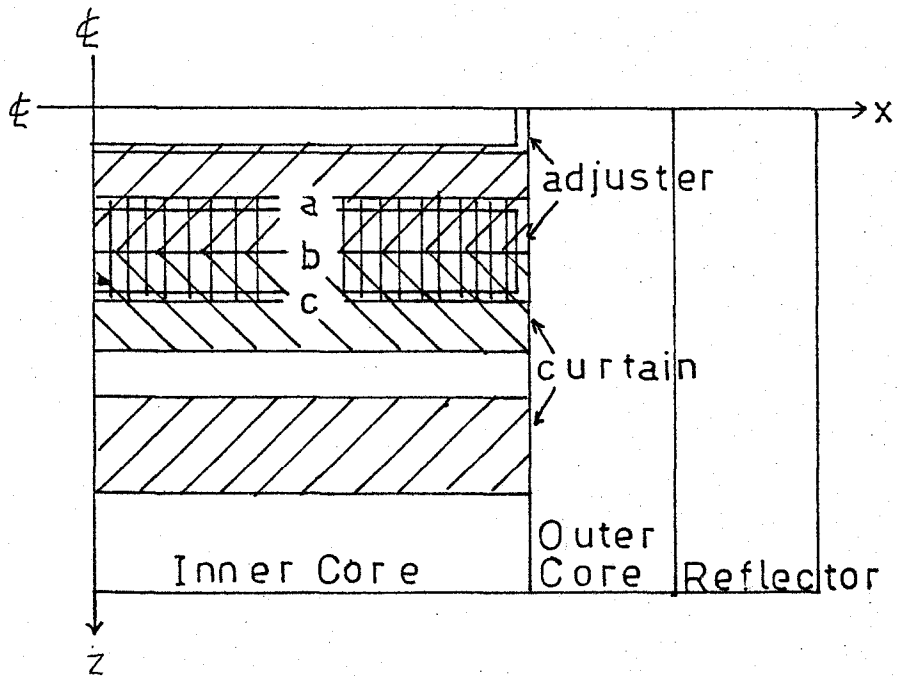

CASE	$\Delta\rho$ (mk)	$\bar{\phi}_2/\phi_{2max}$
ref	———	0.7090
* a	-81.550	0.1915
b	-76.460	0.1756
c	-60.896	0.1951

FIG. 17 SOR CURTAIN STUDY.
ADJUSTED CORE: LAYOUT 6

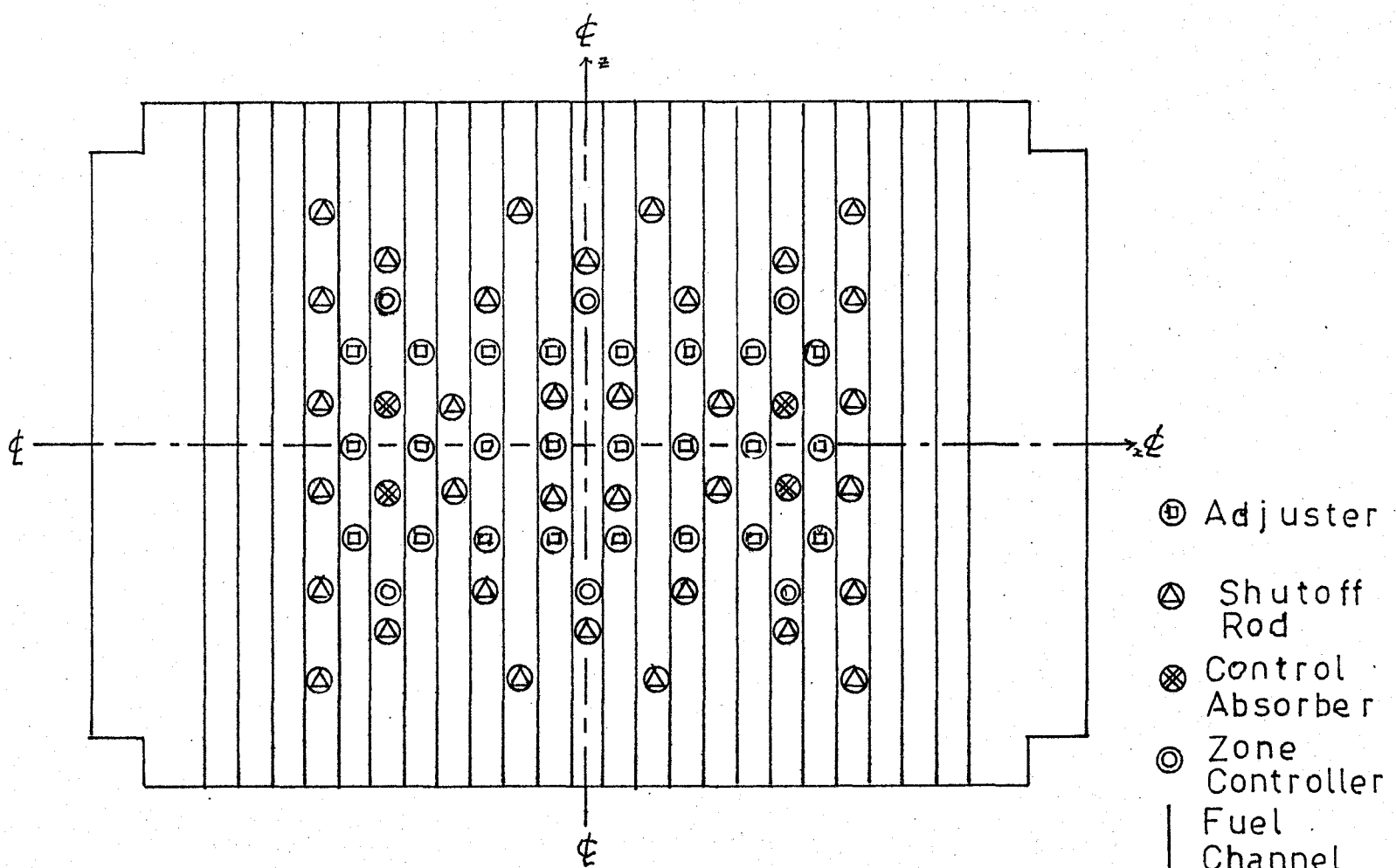

FIG. 18 REACTOR A CORE LAYOUT

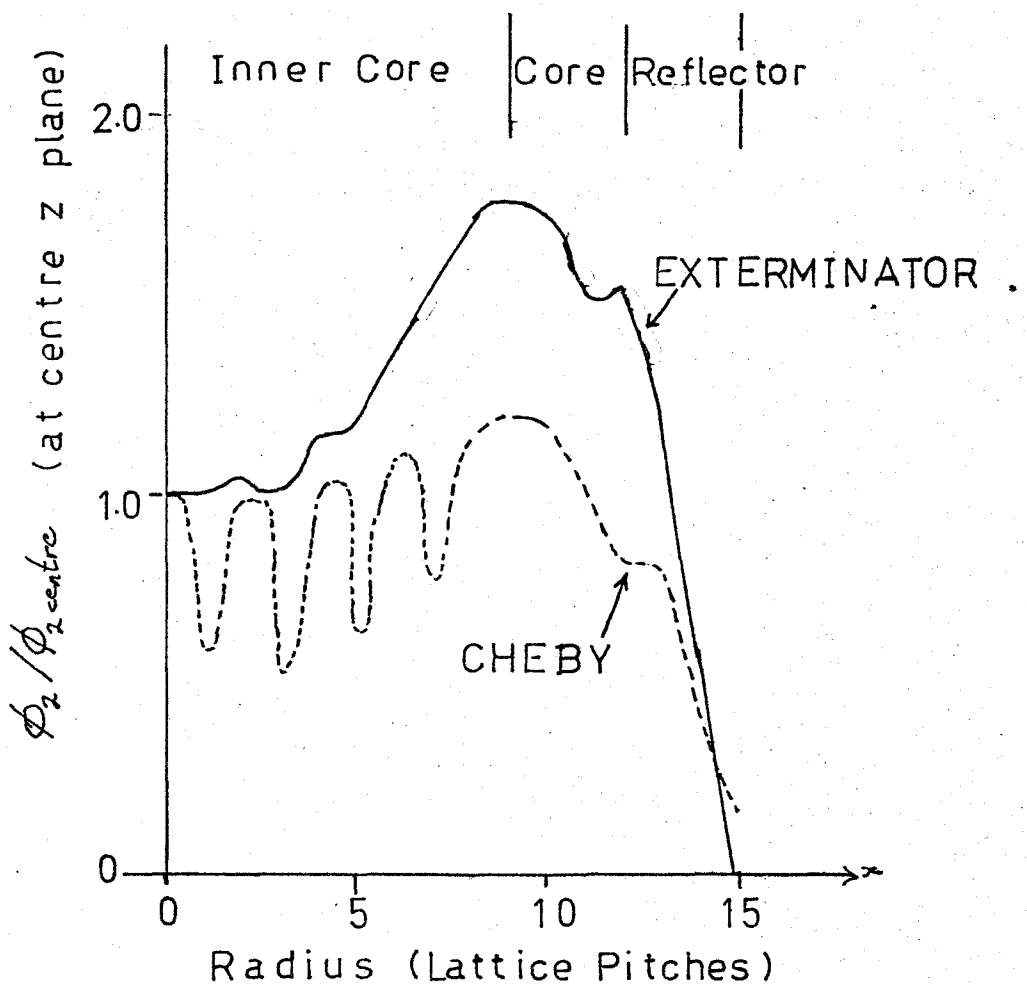

FIG. 19 CHEBY vs EXTERMINATOR
$\phi_2/\phi_{2\,centre}$. SOR OUT

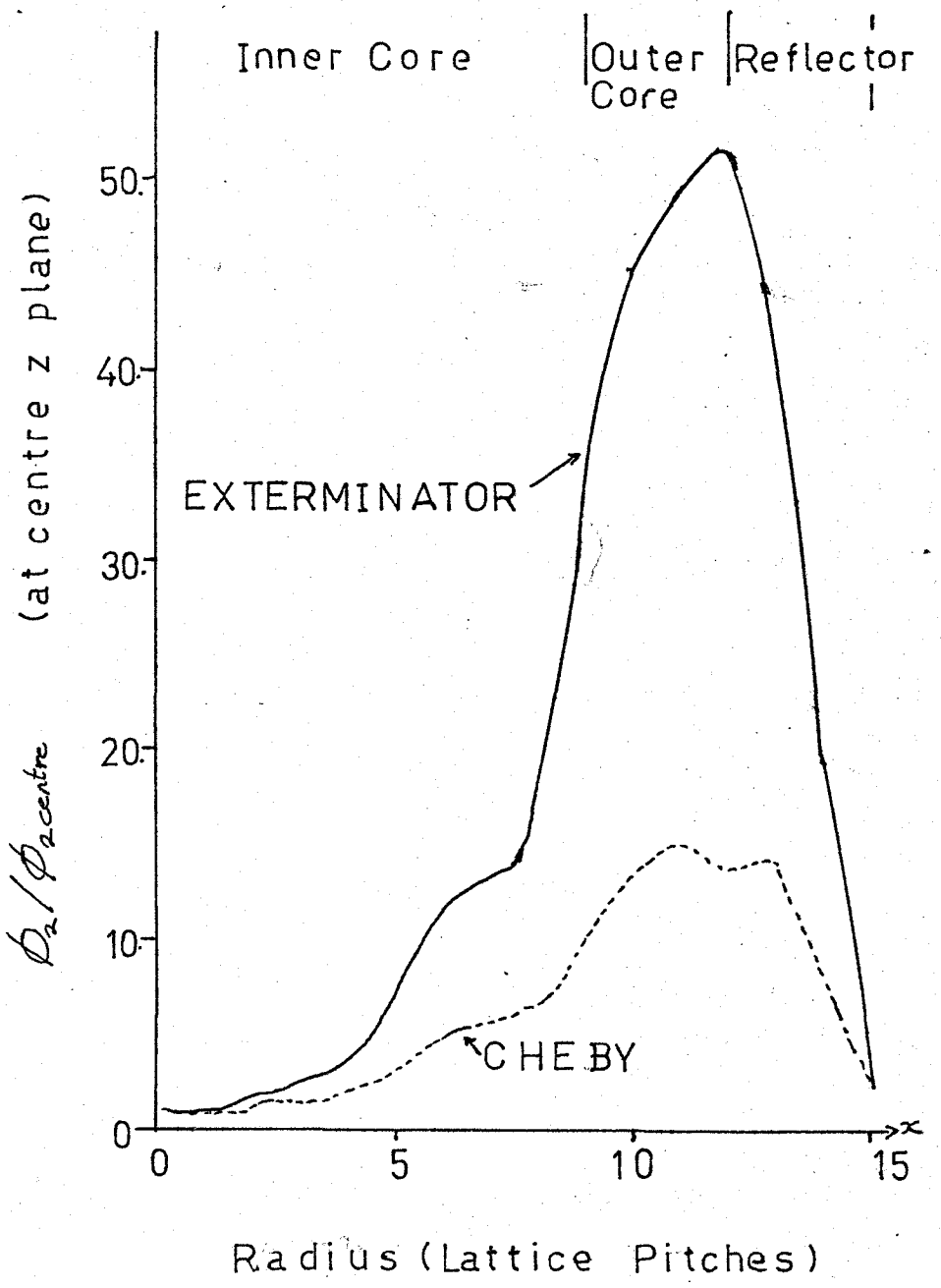

FIG. 20 CHEBY vs EXTERMINATOR
$\phi_2/\phi_{2\,centre}$, SOR IN

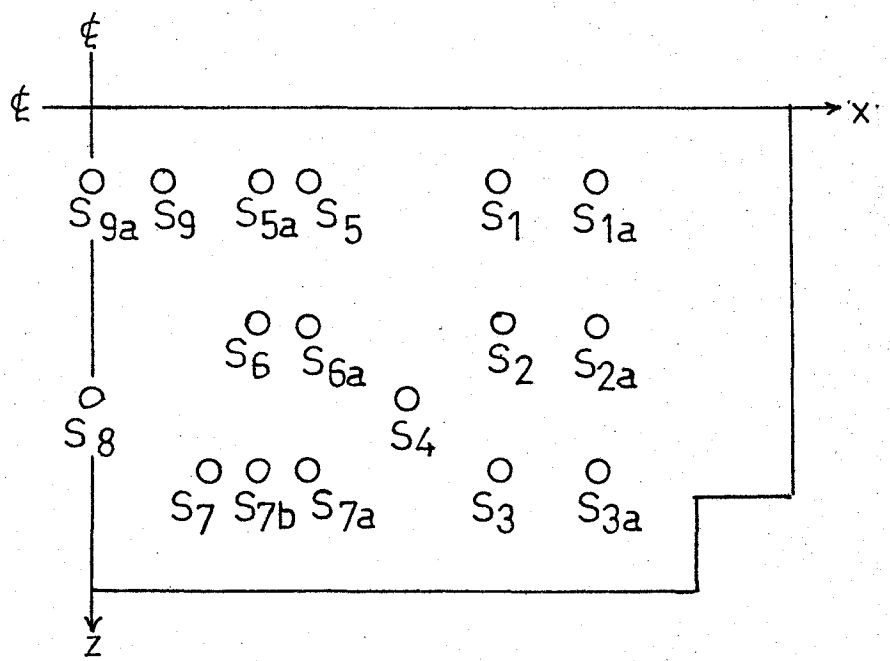

CASE	SOR POSITIONS	$\Delta\rho$ (mk)
1	$S_1, S_2, S_3, S_4, S_5, S_6, S_7 S_8, S_9$	-66.496
2	$S_1, S_2, S_3, S_4, S_5, S_6, S_7, S_8$	-66.120
3	$S_1, S_2, S_3, S_4 S_5, S_6, S_7, S_9$	-66.416
4	$S_1, S_2, S_3, S_4 S_5, S_6, S_7$	-65.743
5	$S_1, S_2, S_3, S_4, S_5, S_6$	-59.899
6	$S_1, S_2, S_3, S_4, S_5, S_6, S_{7a}$	-65.059
7	$S_1, S_2, S_3, S_4, S_5, S_{6a}, S_{7a}$	-58.649
8	$S_1, S_2, S_3, S_4, S_{5a}, S_6, S_{7b}$	-65.082
9	$S_{1a}, S_{2a}, S_{3a}, S_4, S_{5a}, S_6, S_{7b}$	-79.095
10	$S_1, S_2 S_3, S_4, S_5, S_{6a} S_{7a}, S_8, S_{9a}$	-66.702

FIG. 21 REACTOR A CONSTANT B^2 MODEL SOR POSITIONS AND RESULTS

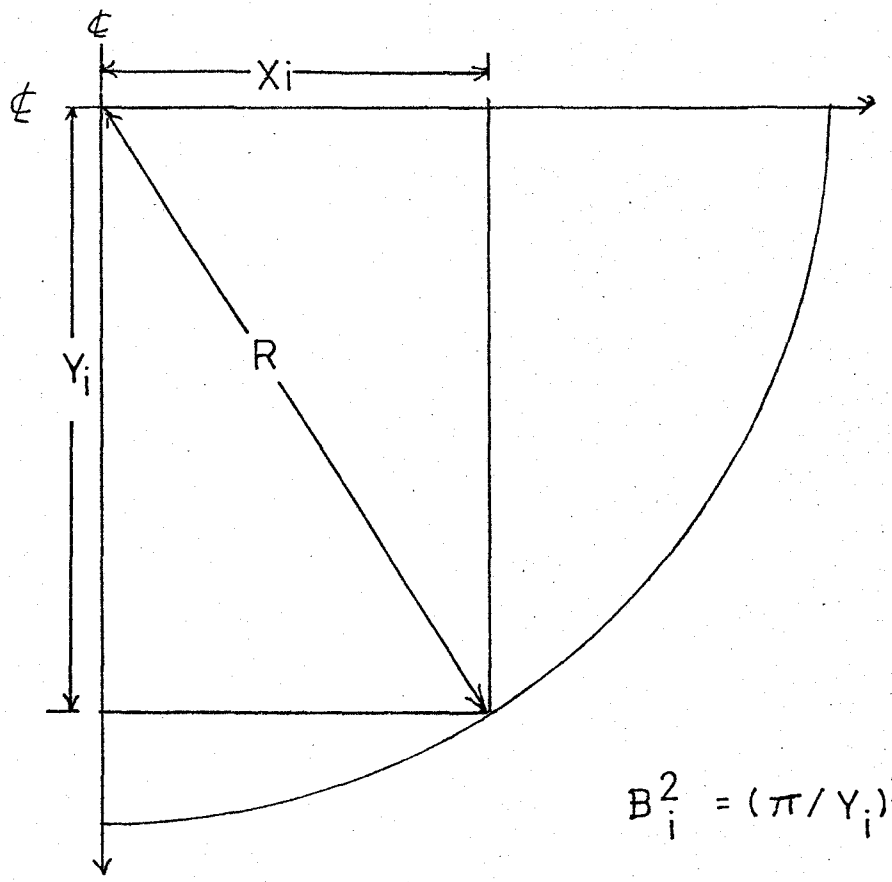

Xi (Pitches)	3·5	5·5	7·5	9·0	11·0	12·0	13·0	14·0	15·0
B_i^2 (m^{-2})	·53	·56	·62	·73	·90	1·1	1·4	2·0	3·9

FIG. 22 VARIABLE BUCKLING CALCULATION

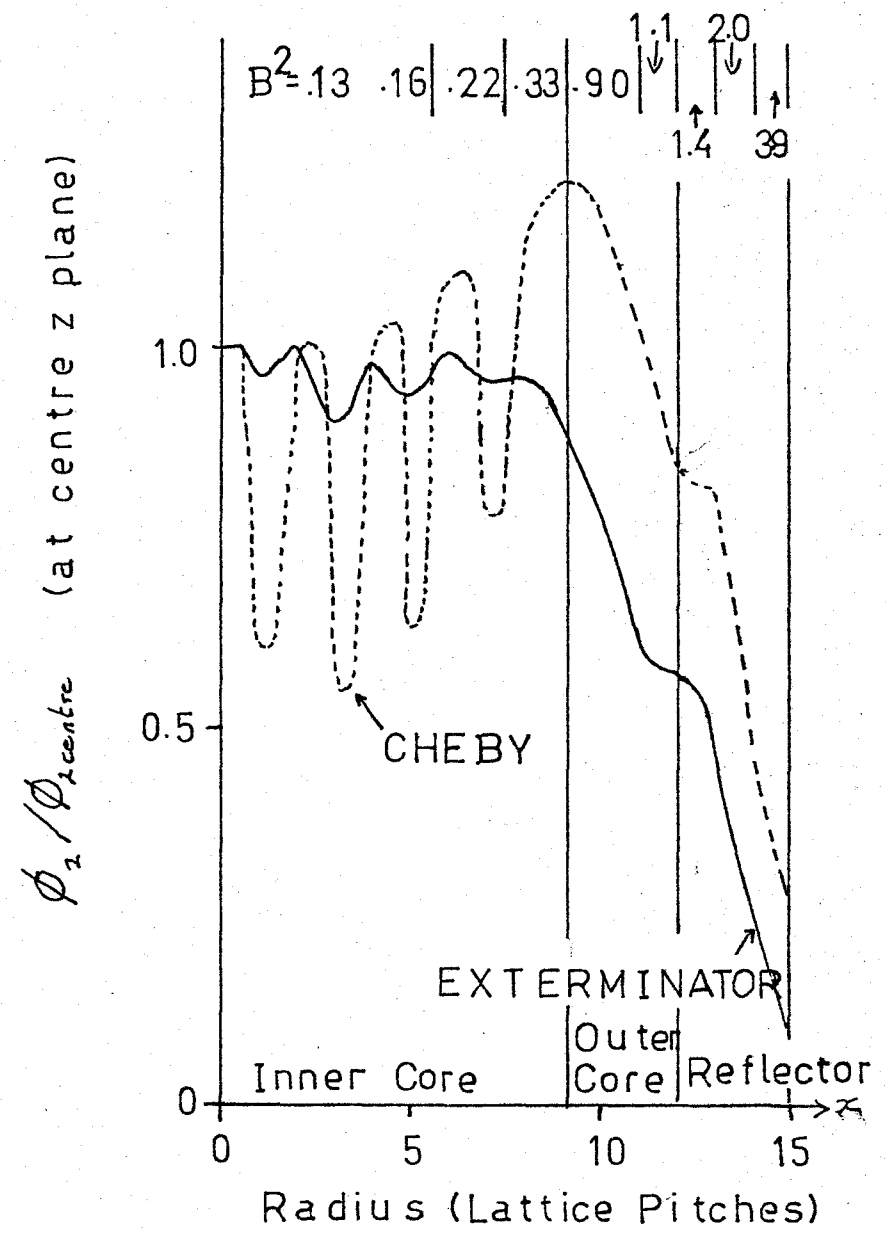

FIG. 23 REACTOR A VARIABLE B^2
RADIAL FLUX, SOR OUT

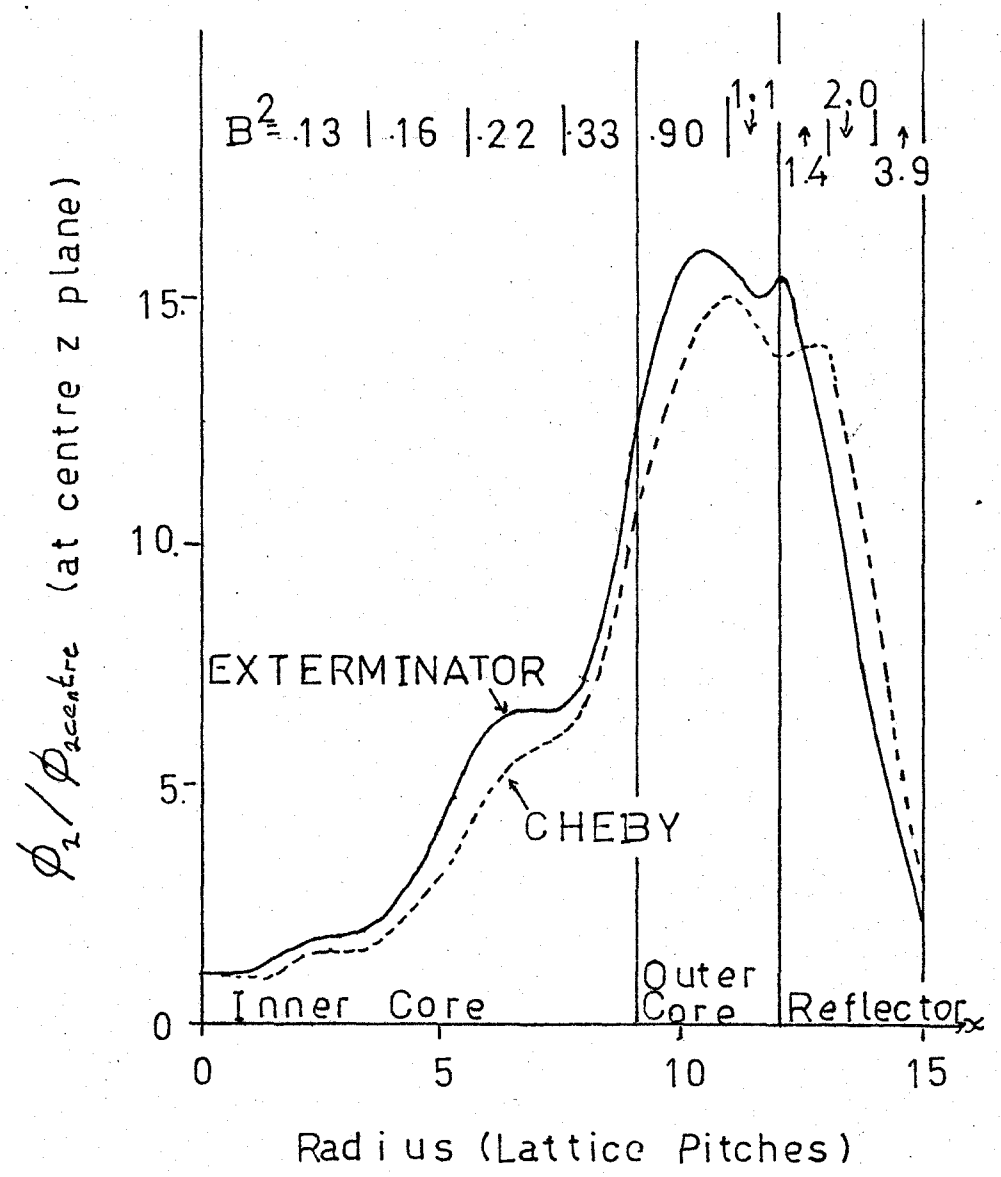

FIG. 24 REACTOR A VARIABLE B^2 RADIAL FLUX, SOR IN

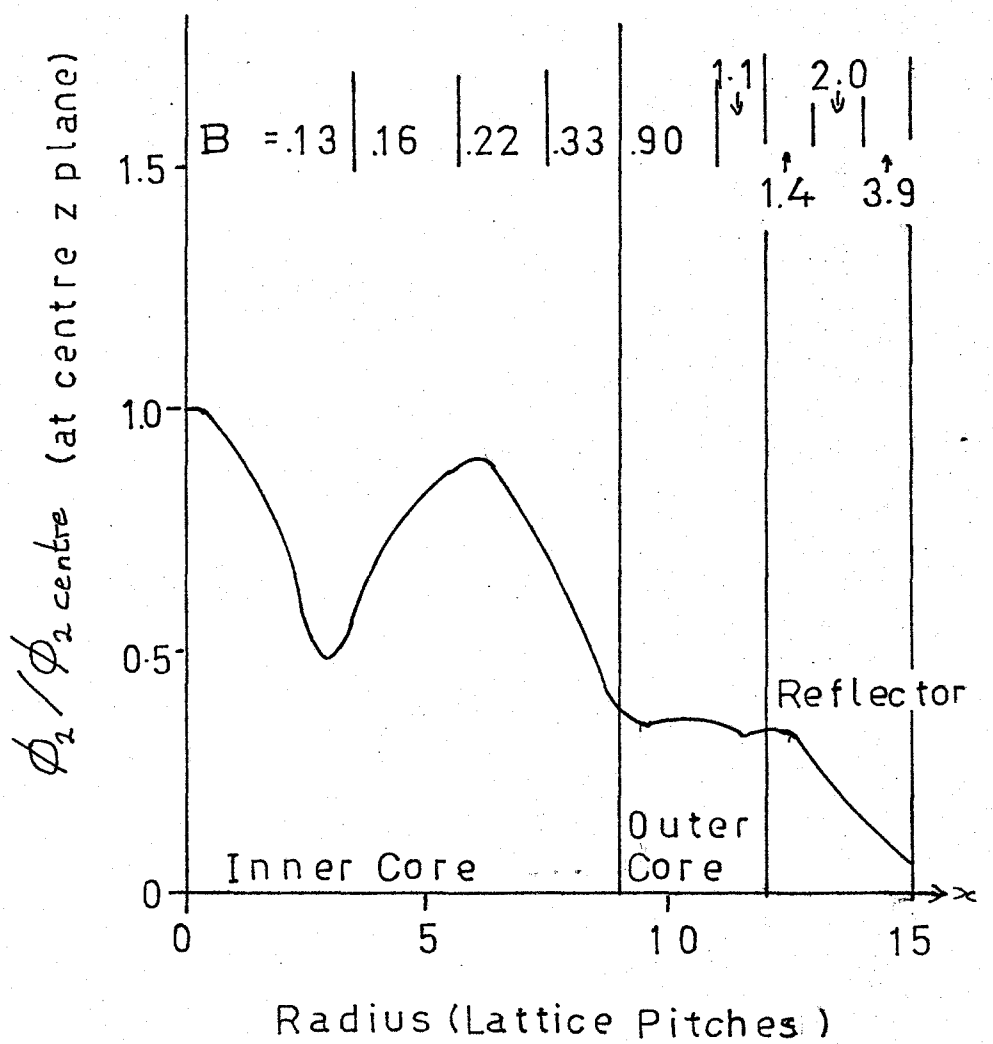

FIG. 25 REACTOR A VARIABLE B^2
SOR IN, 5 PITCH SEPARATION

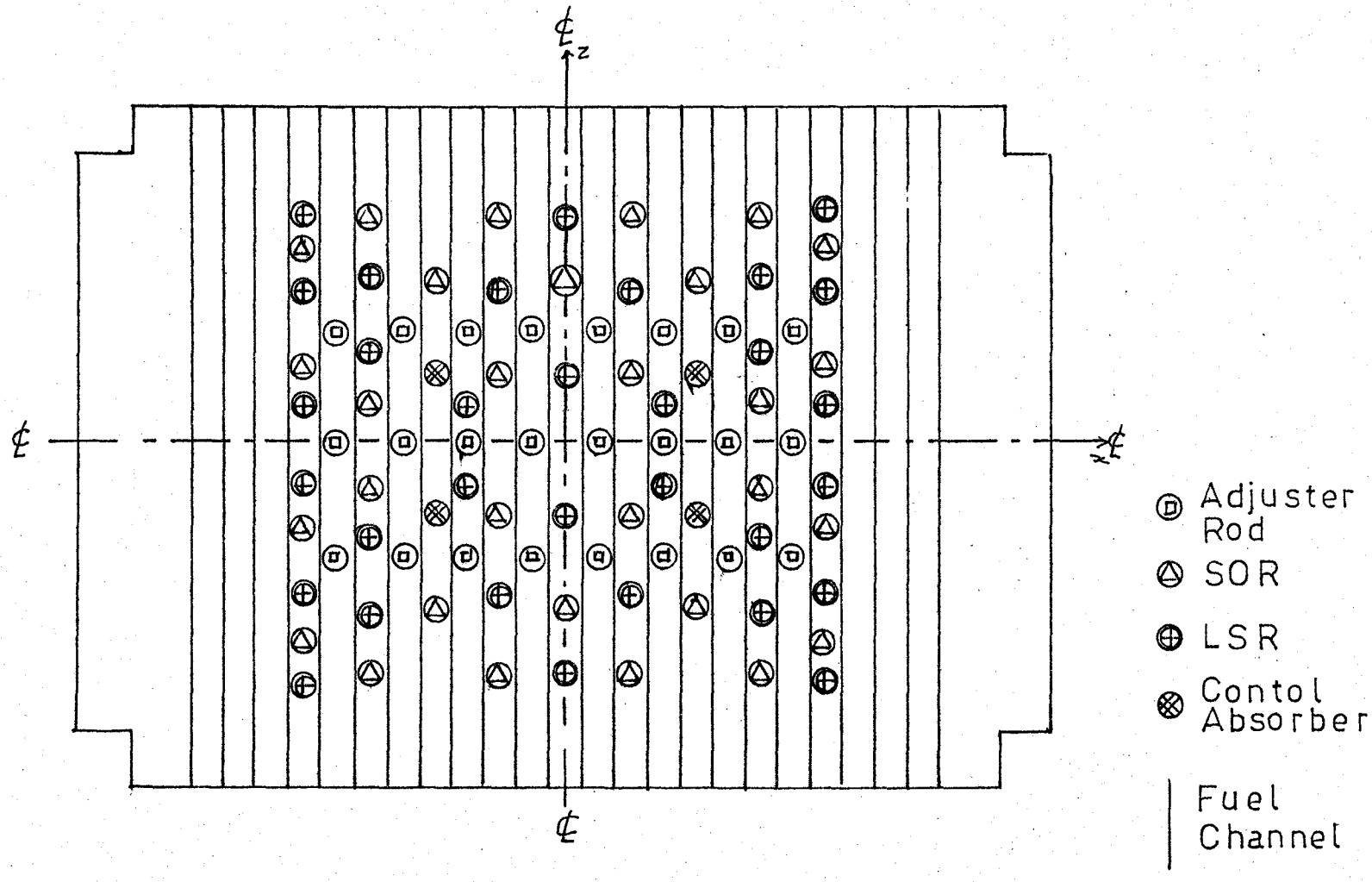

FIG. 26 REACTOR B CORE LAYOUT

REFERENCES

1. E.M. Yaremy, "Reactor and Station Control", Nuclear Energy Symposium, 1974 Conference CNA/AECL, Montreal, Canada.
2. N. Bradley, D.J. Dawson and F.G. Johnson, "Engineering Design of SGHWR's", Proceedings of the Conference held at the Institute of Civil Engineers, 14-16 May, 1968, British Nuclear Energy Society.
3. W.F. Kirtley and M.K. Shaw, "Fast Acting Liquid Shutdown Systems", Institution of Mechanical Engineers Symposium, 18 May, 1967, Some Engineering Aspects of the Winfrith Steam Generating Heavy Water Reactor, London.
4. J.D. Sainsbury, "Accident Analysis", Nuclear Energy Symposium, 1974 Conference - CNA/AECL, Montreal, Canada.
5. J.R. Lamarsh, Introduction to Nuclear Reactor Theory, Addison-Wesley Publishing Co. Inc., Reading, Massachusetts (1972).
6. A.A. Harms and S.I. Schreiner, "An Expository Derivation of Neutron Transport Equations", Nuclear Technology, 11, 144 (1971).
7. E.P. Wigner, "Mathematical Problems of Nuclear Reactor Theory", Proceedings of 11th Symposium in Applied Mathematics of the American Mathematical Society, 23-25 April, 1959.
8. P.F. Zweifel, Reactor Physics, McGraw-Hill Book Co., Toronto (1973).
9. T.B. Fowler, M.L. Tobias and D.R. Vondy, "EXTERMINATOR -A Multigroup Code for Solving Neutron Diffusion Equations in One and Two

Dimensions", ORNL-TM-842, February (1965).

10. T.B. Fowler, M.L. Tobias and D.R. Vondy, "EXTERMINATOR-2: A FORTRAN IV Code for Solving Multigroup Neutron Diffusion Equations in Two Dimensions", ORNL-4078, April (1967).

11. M.L. Tobias and T.B. Fowler, "The EQUIPOSE Method - A Simple Procedure for Group-Diffusion Calculations in Two and Three Dimensions", Nuclear Science and Engineering, 12, 513 (1962).

12. R.S. Varga, Matrix Iterative Analysis, Prentice-Hall, Inc., Englewood, N.J. (1962).

13. Contents of Section 6 are contained in various A.E.C.L. Power Projects internal documents, May-Sept., 1975.